Cardiovascular MR Imaging at 3 T: Opportunities, Challenges, and Solutions[1]

Prabhakar Rajiah, MD, FRCR
Michael A. Bolen, MD

Abbreviations: BOLD = blood oxygen level–dependent, CNR = contrast-to-noise ratio, ECG = electrocardiography, FSE = fast spin echo, GRE = gradient echo, SAR = specific absorption rate, SNR = signal-to-noise ratio, SPIO = superparamagnetic iron oxide, SSFP = steady-state free precession, TE = echo time, 3D = three-dimensional, TR = repetition time

RadioGraphics 2014; 34:1612–1635

Published online 10.1148/rg.346140048

Content Codes: CA MR

[1]From the Cardiothoracic Imaging Section, Department of Radiology, University Hospitals Case Medical Center, Case Western Reserve University School of Medicine, 11100 Euclid Ave, Cleveland, OH 44106 (P.R.); and Cardiovascular Imaging Laboratory, Imaging Institute, Cleveland Clinic Foundation, Cleveland, Ohio (M.A.B.). Presented as an education exhibit at the 2013 RSNA Annual Meeting. Received February 21, 2014; revision requested May 21 and received June 25; accepted July 1. For this journal-based SA-CME activity, the authors, editor, and reviewers have disclosed no relevant relationships. **Address correspondence to** P.R. (e-mail: *radprabhakar@gmail.com*).

SA-CME LEARNING OBJECTIVES

After completing this journal-based SA-CME activity, participants will be able to:

- Describe the physics involved in cardiac MR imaging at 3 T.
- Recognize the challenges and artifacts associated with 3-T cardiac MR imaging.
- Discuss solutions for the most commonly seen artifacts at 3-T cardiac MR imaging.

See www.rsna.org/education/search/RG.

Scan this code for access to supplemental material on our website.

TEACHING POINTS
See last page

Although 3-T magnetic resonance (MR) imaging is well established in neuroradiology and musculoskeletal imaging, it is in the nascent stages in cardiovascular imaging applications, and there is limited literature on this topic. The primary advantage of 3 T over 1.5 T is a higher signal-to-noise ratio (SNR), which can be used as such or traded off to improve spatial or temporal resolution and decrease acquisition time. However, the actual gain in SNR is limited by other factors and modifications in sequences adapted for use at 3 T. Higher resonance frequencies result in improved spectral resolution, which is beneficial for fat suppression and spectroscopy. The higher T1 values of tissues at 3 T aid in myocardial tagging, angiography, and perfusion and delayed-enhancement sequences. However, there are substantial challenges with 3-T cardiac MR imaging, including higher magnetic field and radiofrequency inhomogeneities and susceptibility effects, which diminish image quality. Off-resonance artifacts are particularly challenging, especially with steady-state free precession sequences. These artifacts can be managed by using higher-order shimming, frequency scouts, or low repetition times. B_1 inhomogeneities can be managed by using radiofrequency shimming, multitransmit coils, or adiabatic pulses. Chemical shifts are also increased at 3 T. The higher radiofrequency results in higher radiofrequency deposition power and a higher specific absorption rate. MR angiography, dynamic first-pass perfusion sequences, myocardial tagging, and MR spectroscopy are more effective at 3 T, whereas delayed-enhancement, flow quantification, and black-blood sequences are comparable at 1.5 T and 3 T. Knowledge of the relevant physics helps in identifying artifacts and modifying sequences to optimize image quality. *Online supplemental material is available for this article.*

Introduction

High-field-strength magnets, especially 3 T, have become established in neuroimaging and musculoskeletal imaging and are increasingly used in abdominal imaging. Many centers now use these devices for cardiovascular magnetic resonance (MR) imaging as well. Optimized clinical cardiovascular MR imaging always involves a balance of signal-to-noise ratio (SNR), spatial resolution, and acquisition time. A 3-T system, with its inherent high SNR, high resonance frequencies, and longer T1, offers opportunities to enhance the quality of cardiovascular MR imaging, which depends on high spatial and temporal

Table 1: Physics of 3-T Cardiac MR Imaging

Factors	Features	Limitations
High SNR	Useful in sequences that require high SNR Trade-off for higher spatial resolution Trade-off for higher temporal resolution Trade-off for shorter acquisition time Improved use of parallel imaging	Actual SNR gain is much lower than theoretical gain Various physical factors decrease SNR Modifications in sequences further decrease SNR
Higher resonance frequency	Higher spectral resolution Improved fat saturation Improved MR spectroscopy Faster phase cycling of spins Useful for opposed-phase imaging Higher radiofrequency power and/or frequency, shorter wavelength	Increased chemical shift artifact Higher SAR B_1 inhomogeneity Spatial variation of flip angles
Tissue relaxation changes		
Longer T1	Useful in MR angiography, tagging, perfusion, delayed enhancement	…
Shorter T2	Minimal effect	…
Shorter T2*	Useful with BOLD sequences Useful with SPIO sequences Improved GRE imaging	Not good for quantifying iron
Stable contrast agent relaxivities	Improved contrast at MR angiography combined with longer T1 of background and native blood pool	…

Note.—BOLD = blood oxygen level–dependent, GRE = gradient echo, SPIO = superparamagnetic iron oxide.

Teaching Point

resolution and rapid image acquisition. However, 3-T systems are not without disadvantages, including higher magnetic field and radiofrequency inhomogeneities; higher incidence of susceptibility, off-resonance, and chemical shift artifacts; and higher radiofrequency deposition resulting in a higher specific absorption rate (SAR). These challenges are amplified at cardiovascular MR imaging, which requires high temporal resolution to accurately capture cardiac motion, has a large associated field of view that amplifies artifacts, results in susceptibility artifacts at the interface with lungs containing air, and uses sequences that require a more homogeneous magnetic field and often have high radiofrequency deposition. These challenges are not insurmountable but require an understanding of the relevant physics to optimize the hardware and sequences. In sum, simply implementing a 1.5-T cardiac MR imaging protocol with a 3-T system is not optimal in most situations.

In this review, we discuss the basic physics of 3-T cardiovascular MR imaging. We then discuss common challenges encountered at 3-T cardiac MR imaging and solutions to these challenges. Finally, we discuss the specific advantages and challenges of 3 T for each cardiac MR imaging sequence and highlight solutions.

Physics of 3-T Cardiac MR Imaging

Teaching Point

Cardiac MR imaging at 3 T results in higher SNR, higher resonance frequency, increased in-phase periodicity, and altered relaxation times, all of which have a substantial effect on the performance and quality of cardiac MR imaging. The physics of 3-T cardiac MR imaging are listed in Table 1.

Higher SNR

MR imaging at 3 T has the potential to achieve a higher SNR. Because the magnetization (B_0) is directly proportional to the magnetic field, a theoretical doubling of SNR would be expected with use of a 3-T device versus a 1.5-T device. This higher SNR is beneficial in sequences with low SNR or can alternatively be traded off to obtain images with higher spatial resolution, higher temporal resolution, shorter acquisition time, or a combination of these factors. Higher spatial resolution improves lesion detectability and decreases some artifacts, whereas shortened acquisition time improves patient compliance and reduces motion artifacts. In addition, higher SNR improves the use of parallel imaging, which is usually associated with a decrease in SNR.

The actual increase in SNR at 3 T is lower than the expected doubling: SNR is increased by approximately 1.8-fold with spin-echo and

1.6- to 1.7-fold with GRE sequences (1,2). This is because of the dependence of SNR not only on field strength but also on several other parameters. Physical causes of lower SNR are altered relaxation times such as longer T1 and shorter T2*, B_0 and B_1 inhomogeneities, and susceptibility effects. Spatial resolution, bandwidth, radiofrequency coil availability, and type of image acquisition also affect SNR. Technical modifications made to sequences to compensate for the challenges of 3 T may also result in lower SNR (ie, parameter-induced causes). For example, to reduce the SAR in a steady-state free precession (SSFP) sequence, the flip angle is decreased or the repetition time (TR) is increased, both of which result in lower SNR, with the latter also causing greater susceptibility effects.

Increased Resonance Frequency

Resonance frequency is also directly proportional to the field strength, as $v = \omega/2\pi$, and $\omega = \gamma B_0$ (v = resonance frequency, ω = angular velocity of spin precession, γ = gyromagnetic ratio). At 3 T, the resonance frequency is doubled to 127.8 MHz from 63.9 MHz. One of the benefits of higher resonance frequency is higher spectral resolution, or higher separation between the resonance frequencies of fat and water protons (ie, 450 Hz at 3 T compared with 225 Hz at 1.5 T) (3). This improves the performance of spectral fat-saturation sequences, as inaccurate suppression of water signal does not occur. Similarly, MR spectroscopy is improved at 3 T because of higher separation between the frequencies of various compounds. A disadvantage associated with a higher resonance frequency is a more pronounced chemical shift artifact at fat-tissue interfaces.

Higher resonance frequencies require higher radiofrequency power and/or frequency to stimulate these protons. This means that the radiofrequency coils at 3 T must be tuned to different frequencies than at 1.5 T. The higher radiofrequency pulses result in a shorter wavelength at 3 T than at 1.5 T (26 cm vs 54 cm). This results in a higher amount of radiofrequency absorbed by body tissue, which leads to tissue heating. Shorter wavelengths also result in short-wavelength penetration artifacts. Inhomogeneous penetration of radiofrequency through tissue leads to B_1 inhomogeneity and spatial variation of flip angles.

Higher In-Phase Periodicity

Another effect of higher resonance frequency is the faster phase cycling of spins, which results in a decrease of in-phase periodicity (time until fat and water protons precess in phase) from 4.6 msec at 1.5 T to 2.5 msec at 3 T. At 1.5 T, in-phase sequences are performed at 4.4 msec, while out-of-phase sequences are performed at 2.2 msec. With 3 T, in-phase sequences can be performed at 2.2 msec, while out-of-phase sequences can be performed at 1.1 msec. This is advantageous for sequences that are based on opposed phase (time of flight) because at 3 T these sequences can be performed at a much lower echo time (TE), which results in fewer artifacts as well as reduced acquisition time. However, 3 T is not particularly advantageous for sequences that rely on an exact in-phase setting (ie, dynamic subtraction MR imaging) because there is a short time difference between the in-phase and out-of-phase settings. Small variations may result in out-of-phase acquisition, which is not desirable (4). However, because opposed-phase sequences are used only rarely in cardiac MR imaging, this is not a major limitation.

Changes in Relaxation Times

T1 is 30% longer at 3 T than at 1.5 T (4). The T1 change is tissue dependent; for example, myocardial T1 increases by 12%–42%, whereas blood T1 increases by 7%–40% (5). T1 of myocardium is 1007 msec ± 30 at 1.5 T versus 1220 msec ± 70 at 3.0 T, while that of blood is 1580 msec ± 130 at 1.5 T versus 1660 msec ± 60 at 3 T. The higher difference in myocardium than in blood is due to higher free water and shorter molecular correlation time in blood (5). Longer T1 is useful in several sequences, especially those that are T1 based. For example, grid lines persist longer in myocardial tagging, which enables evaluation of more cardiac cycle phases than at 1.5 T. Longer T1 also improves perfusion imaging by increasing the contrast between normal and hypoperfused myocardium and likewise improves delayed-enhancement imaging by increasing the contrast between normal and infarcted or scarred myocardium. MR angiography is also improved at 3 T because of the lower signal intensity of background tissues as a result of longer T1. High T1 is a disadvantage in SSFP sequences, in which the signal depends on the T2/T1 ratio.

T2 is approximately 15% shorter at 3 T than at 1.5 T, depending on the type of tissue (4). In one study, myocardial T2 was 35 msec ± 4 at 1.5 T and 32 msec ± 2 at 3.0 T, while blood T2 was 290 msec ± 30 at 1.5 T and 275 msec ± 50 at 3.0 T (6). However, these effects are not usually significant at 3 T. T2* is also shorter at 3 T, usually by approximately 50% (6). This shorter T2* is useful with BOLD and SPIO sequences, as both of these sequences depend on T2* effects. However, susceptibility effects may degrade BOLD sequence results, and the lower baseline T2* may diminish the increased T2* effect with SPIO sequences (4). GRE imaging is improved at 3 T, including visualization of myocardial iron.

Table 2: Common Challenges and Artifacts at 3-T Cardiac MR Imaging

Artifact	Physics	Solutions
B_0 inhomogeneity	Higher inhomogeneity by 2 ppm	B_0 calibration map Maximum gradient output
Off-resonance band and flow artifacts	Resonance frequency shifts due to susceptibility gradients	B_0 calibration map Volume-selective higher-order shimming Maximum gradient output Frequency scout and iterative frequency shift Shorter TR Wide-band SSFP GRE sequence
Susceptibility artifact	Higher B_0 inhomogeneities and shorter T2*	Change readout direction Decrease voxel size Shorter TE Highest bandwidth Spin-echo sequence Shim (additional shim coils, new shimming algorithms, higher-order shimming) Parallel imaging Reconstruction algorithms
B_1 inhomogeneities	Higher resonance frequencies and shorter wavelength, amplified by "standing-wave" effect	Multichannel transmit coils Radiofrequency shimming Combined transmit and receive shimming Shorter radiofrequency pulse Higher bandwidth Shorter TR Lower resolution Adiabatic pulses
Dielectric effects	Dielectric effect in conductive medium such as pleural effusion or ascites	Off-resonance coil between transmission coil and patient Radiofrequency cushions or dielectric pads
Chemical shift	Shifting of spatial position of pixels containing fat and water due to higher resonance frequencies	Switch frequency-encoding direction Higher bandwidth Spectral fat saturation Water excitation Inversion nulling
SAR	Higher radiofrequency power	Limit pulses with rapid switching Reduce flip angle Longer TR Parallel imaging Refocusing flip-angle modulation techniques Variable-rate selective excitation

However, the shorter T2* results in poor quantification of iron at 3 T due to the more rapid decay and technical limitations associated with acquiring a very short echo sequence (7).

The relaxivity of the contrast agent (gadolinium chelate) remains relatively constant from 1 T to 5 T (4). However, the baseline T1 of the blood pool is longer at 3 T; hence, the difference between the nonenhanced and contrast-enhanced blood pool is significantly greater at 3 T than at 1.5 T. This factor, in combination with the higher T1 of background tissue, leads to improved contrast-enhanced MR angiography at 3 T, which allows for a decrease in the contrast agent dose or a higher contrast-to-noise ratio (CNR) at the same dose.

Challenges of 3-T Cardiac MR Imaging

Teaching Point

The challenges of 3-T cardiac MR imaging include B_0 inhomogeneities and consequent band, flow, and susceptibility artifacts; B_1 inhomogeneities and consequent field-focusing and dielectric resonance effects; and chemical shift artifacts. These challenges are summarized in Table 2.

B_0 Inhomogeneities

B_0 (static magnetic field) inhomogeneities are greater at 3 T than at 1.5 T, by 2 ppm (Fig 1). This, along with a higher resonance frequency, means that the protons are precessing at different frequencies in the imaging field, which

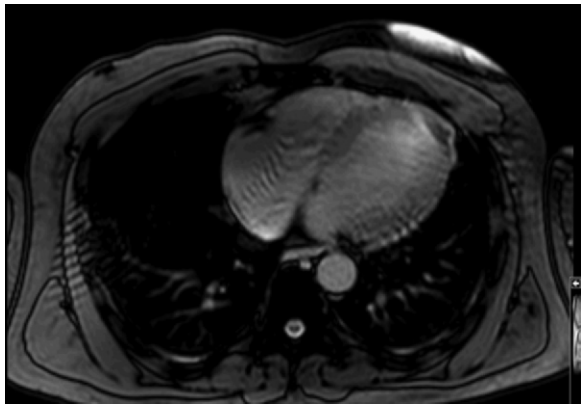

Figure 1. B_0 inhomogeneities. Axial SSFP MR image through the heart shows the effects of static field inhomogeneities, which result in heterogeneous signal intensity and artifacts in the heart. These artifacts can be suppressed with higher-order volume-selective shimming.

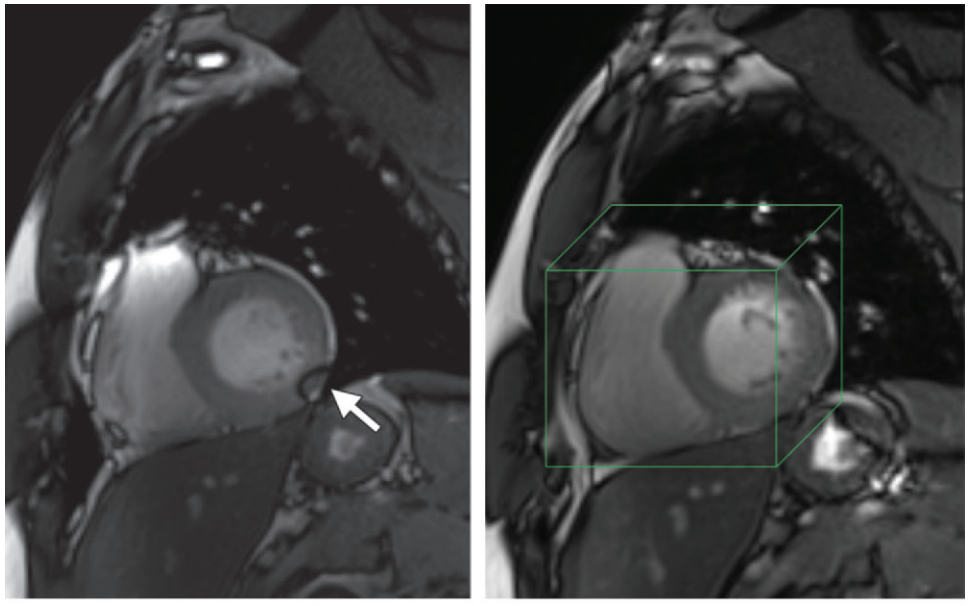

a. **b.**

Figure 2. Off-resonance band and correction with higher-order volume-selective shimming. **(a)** Short-axis SSFP MR image shows a band artifact at the inferolateral wall of the left ventricle, at the interface between the left ventricle and the diaphragm adjacent to the lung (arrow). **(b)** Short-axis SSFP MR image with application of higher-order volume-selective shimming (green box) over the cardiac chambers shows elimination of the off-resonance band seen in **a** from the area of interest.

makes the performance of sequences that require a homogeneous magnetic field (eg, SSFP) challenging. Artifacts such as band, flow, and susceptibility are also increased at 3 T because of B_0 inhomogeneities. Shorter T2* is another consequence of these inhomogeneities, although this may be beneficial in BOLD applications (as described earlier). Improvements to B_0 inhomogeneities can be realized with volume-selective higher-order shimming. A B_0 calibration map obtained at the beginning of the imaging examination can also improve field homogeneity. Finally, a gradual rather than steep gradient may also ameliorate this problem.

Figure 3. **(a)** Four-chamber SSFP MR image shows extensive off-resonance band and flow artifacts in the apex of the left and right ventricles (arrow). **(b)** Frequency scout map obtained at various resonance frequencies through the same imaging plane as **a** shows different appearances at different frequencies. The frequency map also illustrates how band and flow artifacts vary in appearance and location at different resonance frequencies. From this scout map, the central frequency at which the lowest amount of artifacts is seen is selected. In this case, there is no artifact at 0 Hz. **(c)** Four-chamber SSFP MR image with a resonance frequency of 0 Hz obtained at the same section location as **a** and **b** shows elimination of the flow artifact.

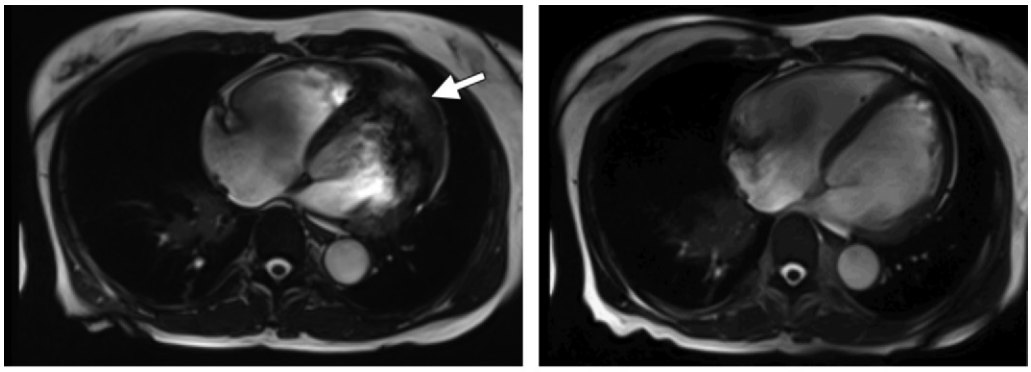

a. c.

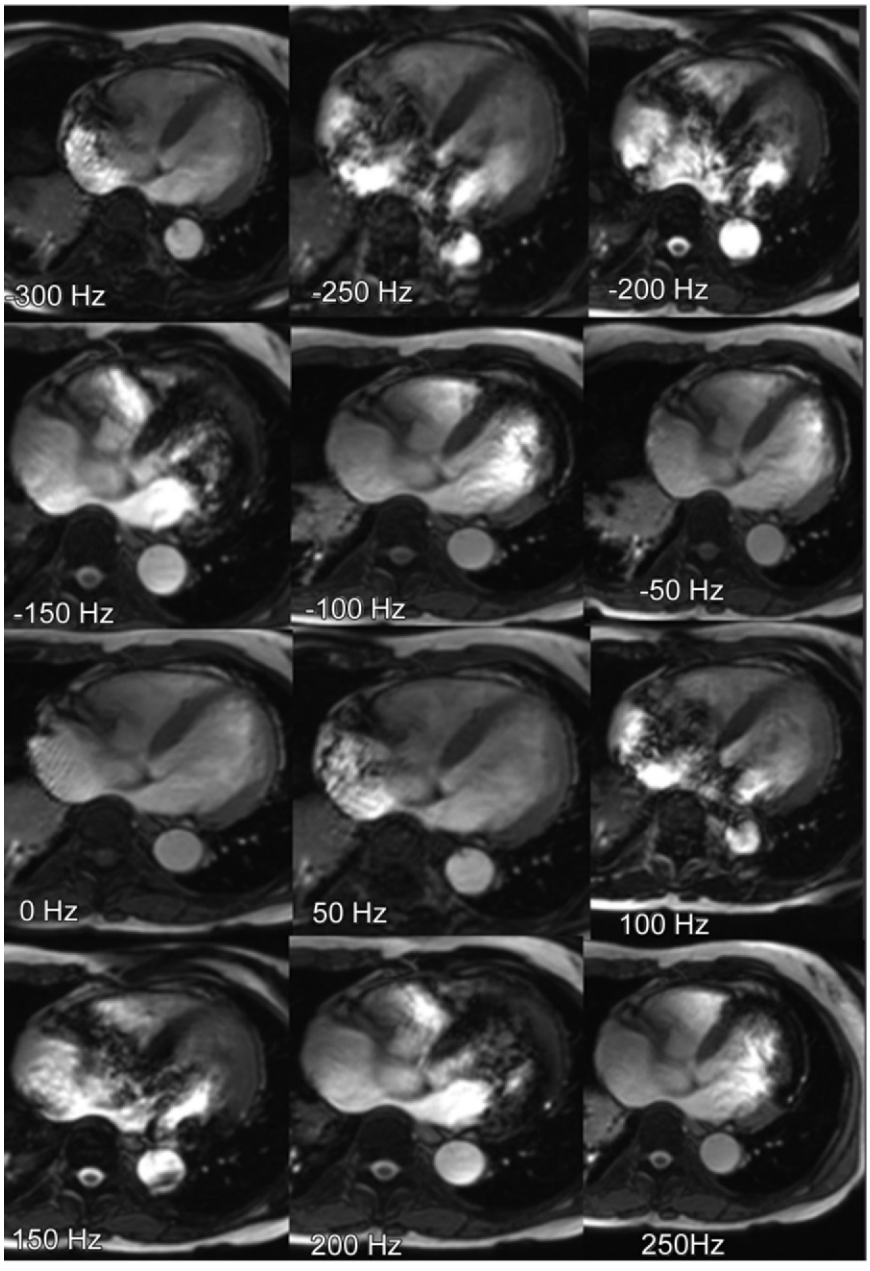
-300 Hz
-250 Hz
-200 Hz
-150 Hz
-100 Hz
-50 Hz
0 Hz
50 Hz
100 Hz
150 Hz
200 Hz
250Hz

b.

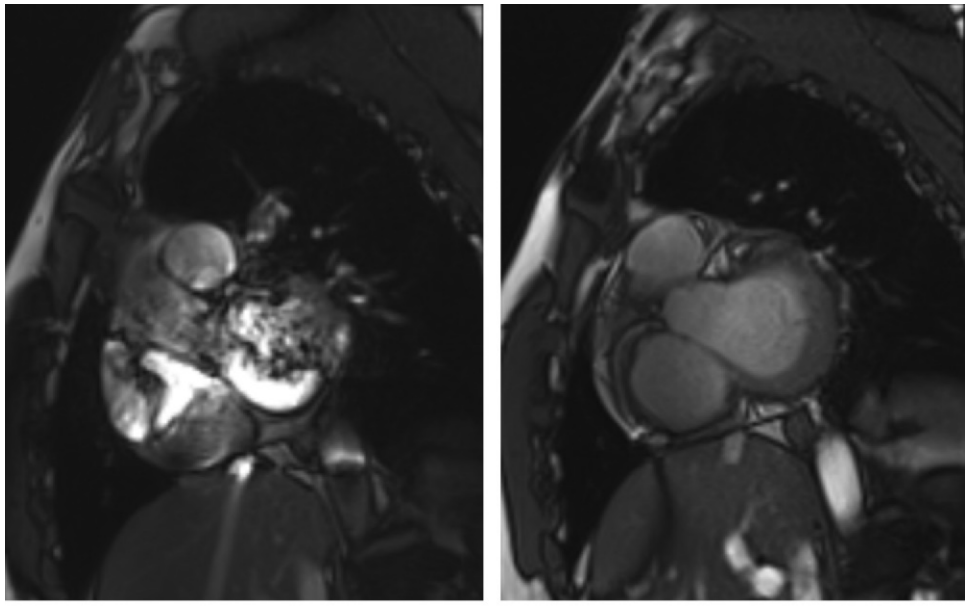

a. b.

Figure 4. Flow artifact and correction. **(a)** Short-axis SSFP MR image through the basal region of the ventricles shows extensive flow artifacts due to a disturbed steady state of magnetization. **(b)** Short-axis SSFP MR image obtained after higher-order shimming and selection of a central frequency using a frequency scout shows elimination of the artifacts.

Band and Flow Artifacts.—Dark band artifacts are due to off-resonance effects (resonance frequency shifts) caused by magnetic susceptibility gradients. These artifacts are seen at frequencies in which there is a transition of signal phase from positive to negative. The appearance and location of band artifacts depend on field strength and susceptibility differences. Band artifacts are more prominent at 3 T and arise closer to the center of the field of view than at 1.5 T. These artifacts are seen at the interface of tissues with high susceptibility differences, such as the myocardium-lung interface adjacent to the inferolateral wall of the left ventricle, the lung-diaphragm interface (Fig 2a), and near the coronary sinus, which contains deoxygenated blood. The effect of the band, which unfortunately can be extensive at 3 T, depends on its location. The distance between bands is inversely proportional to the TR and the slope of the frequency gradient. When an off-resonance band is seen in a cardiac chamber or inflow vessel, the steady state of magnetization is disturbed, resulting in a loss of image contrast, especially with an SSFP sequence.

There are several possible solutions for off-resonance effects. The creation of a more homogeneous magnetic field, a B_0 calibration map, and higher-order volume-selective shimming can decrease artifacts (Fig 2). With a frequency scout (ie, fast low-resolution images obtained at different resonance frequencies), the central frequency can be visually estimated and the optimal frequency offset calculated to obtain a higher-resolution image (8). This requires acquisition of additional images; often, the central frequency varies in different planes, requiring multiple additional scout images in different planes (Fig 3). Use of gradual rather than steep frequency gradients can also help diminish off-resonance effects. Combining a higher-order shim with a frequency scout is often the best solution (Fig 4). Use of a shorter TR increases the distance between bands but also increases the SAR (Fig 5). Use of a wide-band SSFP sequence widens the spacing between dark bands without resonance frequency modification. With this sequence, two alternating repetition times are used with alternating radiofrequency phases. If these methods are not successful, then it may be best to use an alternative sequence such as GRE (eg, fast low-angle shot [FLASH] or fast field echo [FFE]).

Susceptibility Effects.—Susceptibility is the extent of magnetization of a material when it is placed in a magnetic field. The local magnetic field developed by the material modifies the overall magnetic field (diamagnetic, net decrease; paramagnetic, net increase). This may be seen, for example, when there is metal in the imaging field of view and is due to the higher susceptibility of metal compared with soft tissue. Susceptibility artifacts are seen at the interfaces

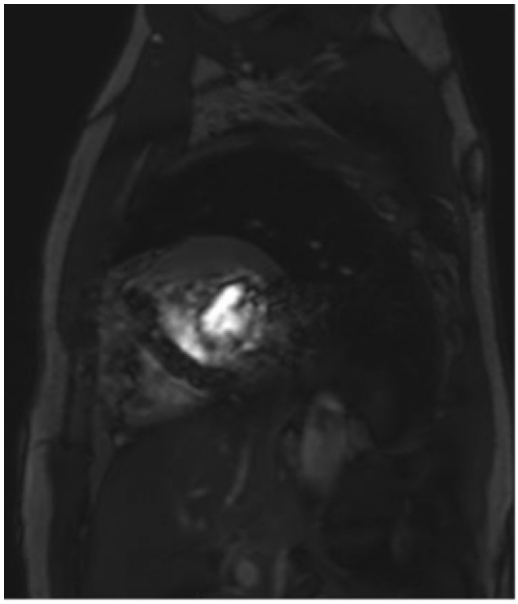

a.

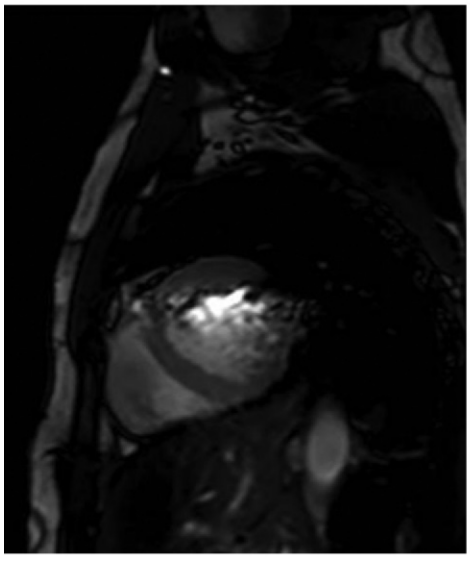

b.

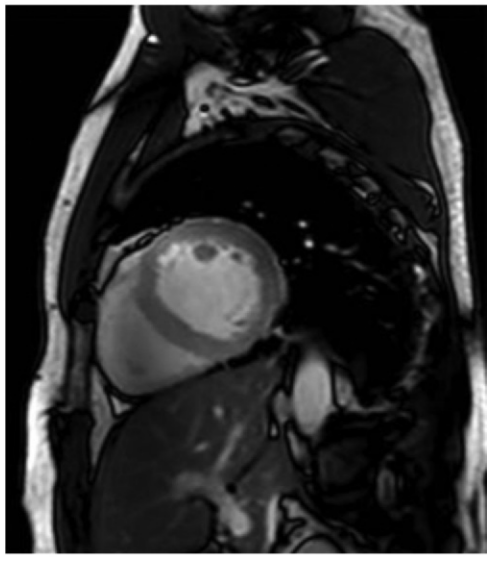

c.

Figure 5. Effect of TR on artifacts. **(a)** Short-axis SSFP MR image (TR = 6.5 msec) shows extensive artifacts and loss of signal in the ventricles. **(b)** Short-axis SSFP MR image (TR = 4.5 msec) at the same section location shows a decrease in the artifact, which has moved to the superior portion of the ventricle, and improved signal intensity. **(c)** Short-axis SSFP MR image (TR = 2.5 msec) at the same section location shows elimination of the artifact and normal signal intensity and contrast between the myocardium and blood pool.

of materials with different magnetic susceptibilities because the imaging computations assume a constant magnetic field, even when it is not. Variations in the local magnetic field and resonance frequencies due to susceptibility result in misregistration of the proton locations, causing variations in signal intensity or distortions. Signal may be cancelled if there is intravoxel dephasing (in a large voxel that contains tissues with different susceptibilities, faster dephasing occurs, resulting in signal loss). Fat suppression is less effective at fat-water and air-tissue interfaces. Susceptibility artifacts vary linearly with the magnetic field and are twice as prominent at 3 T than at 1.5 T because of greater B_0 inhomogeneities and shorter T2*. These artifacts are more prominent with SSFP sequences than with GRE sequences (Fig 6). With SSFP, the phase shift is directly proportional to TR, whereas with GRE, it is directly proportional to TE; because TR is greater than TE, these artifacts are more common with SSFP sequences.

Solutions to susceptibility artifacts include changing the readout direction to move the artifact away from the area of interest, decreasing the voxel size, shortening the TE, and increasing the bandwidth. Further approaches include using shim techniques such as additional shim coils, new shimming algorithms, and higher-order shimming; using parallel imaging, which reduces the length of echo trains and the accumulation of phase errors; and using reconstruction algorithms that correct phase errors periodically (eg, periodically rotated overlapping parallel lines with enhanced reconstruction [PROPELLER]).

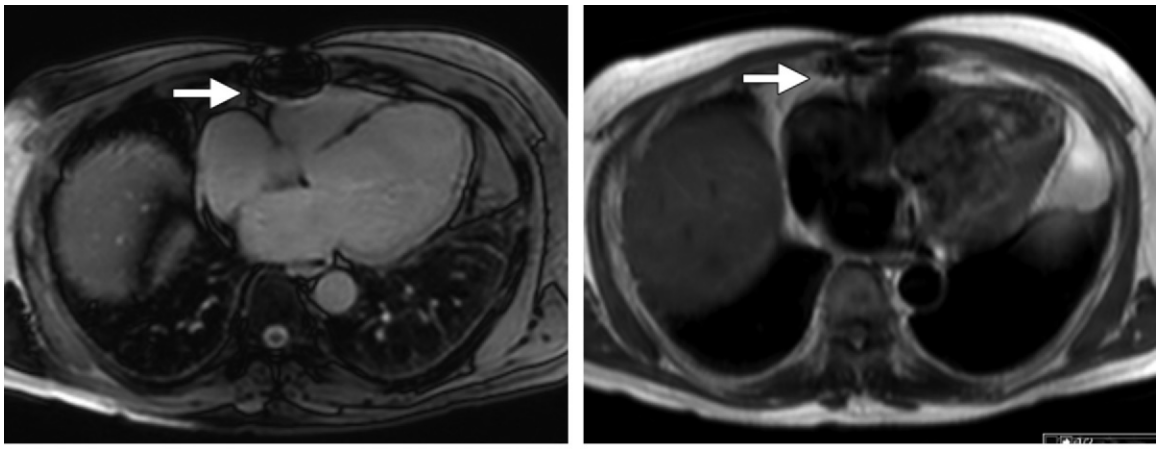

a. b.

Figure 6. Susceptibility artifacts. **(a)** SSFP MR image at 3 T shows a prominent susceptibility artifact from a median sternotomy wire (arrow). **(b)** Half-Fourier acquisition single-shot turbo spin-echo (HASTE; Siemens Healthcare, Erlangen, Germany) MR image shows that the same artifact is less prominent (arrow).

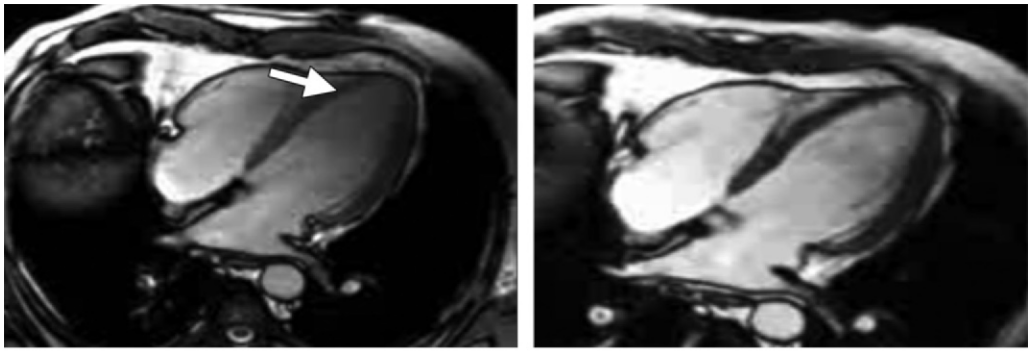

a. b.

Figure 7. B_1 inhomogeneities and shading. **(a)** Four-chamber SSFP MR image shows heterogeneous loss of signal intensity in the apical regions of the cardiac chambers (arrow) because of B_1 inhomogeneities inherent at 3 T. **(b)** Four-chamber SSFP MR image at the same location shows that the addition of a radiofrequency multitransmit coil improves the appearance of dielectric shading.

B_1 Inhomogeneities

As discussed earlier, the radiofrequency pulse at 3 T has a higher frequency than at 1.5 T, which also implies a shorter wavelength (234 cm at 3 T vs 540 cm at 1.5 T, in free space at 128 MHz). The wavelength is further decreased to approximately 26 cm in tissues (4) because of the presence of water, which has a high dielectric constant, thus decreasing the speed and wavelength of the radiofrequency pulse. This low wavelength results in a field-focusing effect (shading) with a maximum B_1 in the center of the body, higher energy deposition, focused and/or higher flip angles, and maximal SNR. Because of eddy currents near the surface of the body, field focusing is less evident at the surface. The B_1 inhomogeneity is further reinforced by the "standing-wave" effect (standing waves generated by the reflection of radiofrequency waves at interfaces with high-conductivity gradients), in which signal variations are seen on images because of destructive interference. This is especially true in large-field-of-view studies, obese patients, and patients with pleural effusions or ascites in the upper abdomen. This B_1 inhomogeneity results in flip-angle variability (as much as 40%) (7,8). Rings of signal intensity loss or shading of signal intensity between superficial and central body parts are noted (Fig 7). These factors may cause heterogeneous suppression of myocardial signal with delayed-enhancement sequences and inadequate T2 preparation with coronary MR angiographic sequences. In addition, a conductive medium such as pleural fluid or ascitic fluid in the upper abdomen may generate electrical current when it interacts with the rapidly changing magnetic field of the radiofrequency pulse (Fig 8). This electrical current in turn generates a magnetic field that opposes the magnetic field of the radiofrequency pulse, thus decreasing the amplitude and energy of the radiofrequency pulse and resulting in further radiofrequency heterogeneity (9).

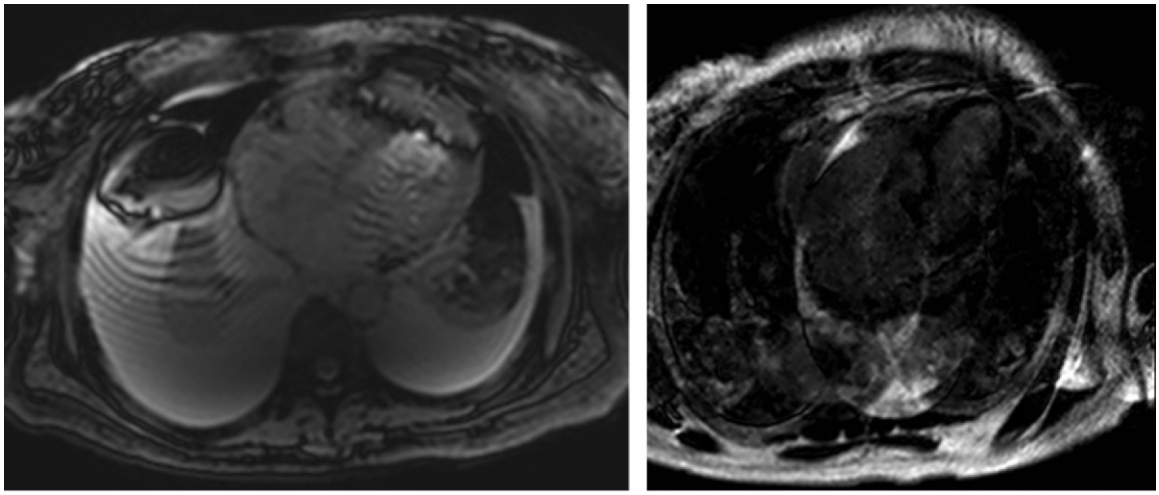

a. b.

Figure 8. Dielectric effects. **(a)** Axial SSFP MR image in a patient with large pleural effusions shows extensive artifacts overlying the heart, findings due to dielectric effects caused by fluid. **(b)** Four-chamber delayed-enhancement image in a patient with bilateral moderate pleural effusions shows extensive artifacts and heterogeneous suppression of the myocardial signal. Solutions include using cushions with high dielectric constants on the anterior chest wall, using an advanced radiofrequency coil design, or repeating MR imaging after thoracentesis.

Solutions for B_1 inhomogeneities include hardware and software modifications. Hardware modifications include a multichannel transmit coil, in which two out of four parameters (phase, amplitude, waveform, and frequency) of the various coil elements can be altered to obtain a homogeneous B_1. Radiofrequency shimming uses multiple radiofrequency transmission sources to compensate for variable flip angles. Alternatively, transmit (B_1) shimming may be combined with receive shimming (Constant Level Appearance [CLEAR]; Philips Medical Systems, Best, the Netherlands); a spiral configuration of coils can modify current patterns and decrease B_1 inhomogeneity. An off-resonance coil placed between the transmission coil and the patient can double as a dielectric, changing radiofrequency transmission. Radiofrequency cushions or dielectric pads, typically containing a gel with a high dielectric constant (mixed with gadolinium), placed on the anterior chest wall can also improve B_1 homogeneity. Use of a shorter radiofrequency pulse, higher bandwidth, shorter TR, and lower resolution may also decrease B_1 inhomogeneity. An adiabatic radiofrequency pulse is another option for decreasing B_1 inhomogeneity (10). Unlike a typical radiofrequency pulse in which the flip angle varies sinusoidally with the radiofrequency power, with an adiabatic pulse, the flip angle stays constant once the radiofrequency pulse reaches a threshold. An additional practical consideration is that in patients with extensive effusions or ascites, cardiac MR imaging may be performed after centesis.

Chemical Shift Artifacts

Chemical shift refers to differences in the resonance frequencies of protons that reside in different molecular environments. For example, the difference between fat and water protons is 225 Hz at 1.5 T and 450 Hz at 3 T. There are two types of chemical shift artifacts. In the first type, spatial misregistrations of pixels containing fat and water are seen at the fat-water interface. These artifacts, which are caused by differences in the resonance frequencies of fat and water, are more common and are twice as wide at 3 T than at 1.5 T because of greater differences in these frequencies. These artifacts are seen only in the frequency-encoding direction, appearing as a hypointense band at the lower part of the gradient and as a hyperintense band at the higher part of the gradient. To overcome these artifacts, the frequency-encoding direction can be switched, eliminating the chemical shift artifact from the area of interest. Another solution is to increase the bandwidth. Although a higher bandwidth lowers SNR, the inherently higher SNR at 3 T compensates for this. A higher bandwidth also allows faster data sampling, which reduces acquisition time and TE and allows a higher number of sections of TR (4). Other techniques include spectral fat saturation, water excitation, and inversion nulling. The second type of chemical shift artifact is due to intravoxel phase cancellation in pixels that contain both fat and water. This type of artifact is seen in all pixels and is not limited to the frequency-encoding direction (Fig 9). These artifacts are

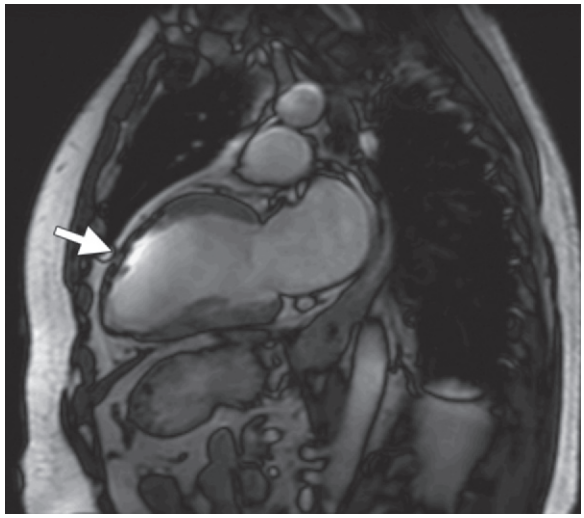

Figure 9. Chemical shift artifact. Two-chamber SSFP MR image shows a chemical shift artifact (arrow), which is seen as a dark band at the interface between the anterior left ventricular myocardium and the pericardial fat.

not more common at 3 T than at 1.5 T. However, the times for in-phase and opposed-phase imaging are different at 3 T compared with at 1.5 T: specifically, at 1.5 T, in phase occurs at 4.4 msec and out of phase occurs at 2.2 msec, while at 3 T, in phase occurs at 2.2, 4.4, and 6.6 msec and out of phase occurs at 1.1, 3.3, and 5.5 msec.

Special Considerations

Parallel Imaging

Parallel imaging is a term used to describe a series of image-acceleration techniques where data are variously undersampled, thereby reducing the acquisition time without sacrificing the desired spatial resolution. In general, these techniques use Fourier-domain or k-space–based algorithms and are used to decrease acquisition time or increase spatial or temporal resolution. However, parallel imaging is limited by signal loss, which is proportional by a factor of the square root of the acceleration factor. Conveniently, 3 T improves the use of parallel imaging, and parallel imaging improves the use of 3 T. The inherently higher SNR at 3 T makes this technique a natural fit for parallel imaging approaches, as a higher degree of acceleration can be used without losing as much signal (Fig 10). In addition, *g*-forces are decreased at 3 T. The higher resonance frequency at 3 T enables greater separation of coils in the frequency domain, thus improving parallel imaging. The higher parallel imaging factors employed at 3 T are used to increase spatial or temporal resolution or to decrease acquisition time at 3 T. Parallel imaging also works synergistically with 3-T imaging by decreasing radiofrequency deposition and SAR, as a lower number of radiofrequency pulses are needed because of undersampling. Parallel imaging also decreases susceptibility effects.

Teaching Point

High SAR

Radiofrequency deposition in tissues results in local tissue heating due to energy transfer from the radiofrequency pulse. This is measured with the SAR, which represents energy absorption per kilogram of body weight per unit of time. Safety standards dictate that this value remains less than 1° C or 4 W/kg averaged over the whole body for 15 minutes. Because SAR and the power required to generate a particular flip angle are directly proportional to the square of the resonance frequency (square of the magnetic field), there is an inherent quadrupling of SAR at 3 T compared with at 1.5 T; hence, the SAR limit is reached more quickly at 3 T. A further increase in SAR is realized with increased flip angle (proportional to the square of the flip angle), shorter TR, larger patient size, positioning the patient in the isocenter of the magnet, coil design, and increased frequency of radiofrequency pulses (eg, fast spin-echo [FSE] and SSFP sequences). The SAR is also higher with sequences that involve rapid switching, such as SSFP and FSE.

To limit SAR, a straightforward solution would be to limit the use of sequences that have a high SAR. However, this is difficult in cardiac MR imaging because SSFP is a critical sequence. The

Figure 10. Parallel imaging. **(a–d)** SSFP MR images at 1.5 T show progressive loss of signal intensity with higher acceleration factors. Acceleration factors are 0 in **a**, 1 in **b**, 2 in **c**, and 3 in **d**. **(e–h)** SSFP MR images at 3 T show no appreciable signal intensity change with higher acceleration factors (1 in **e**, 2 in **f**, 3 in **g**, and 4 in **h**) because of higher SNR reserve and less impact of *g*-factors. ▶

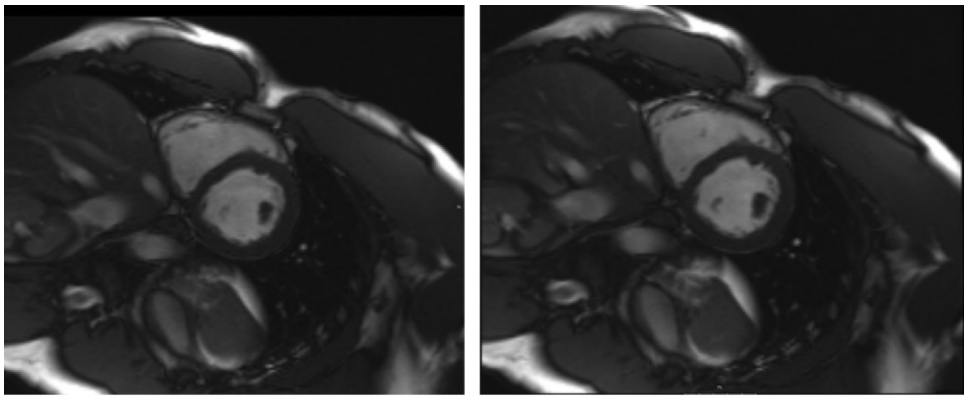

a. b.

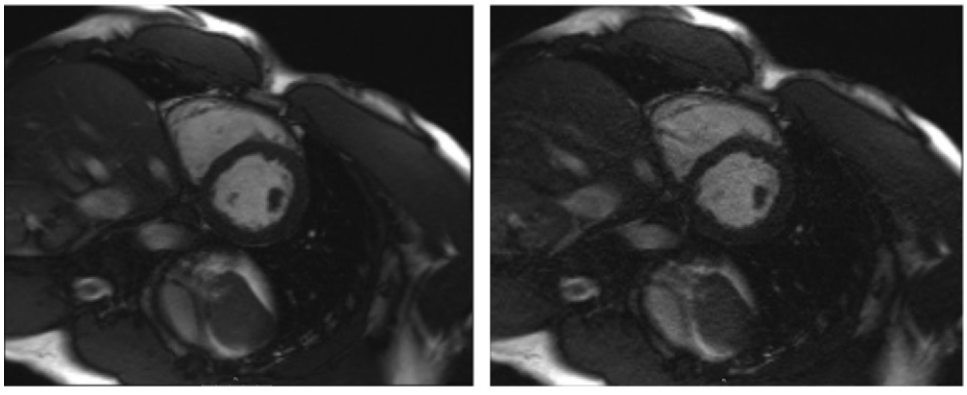

c. d.

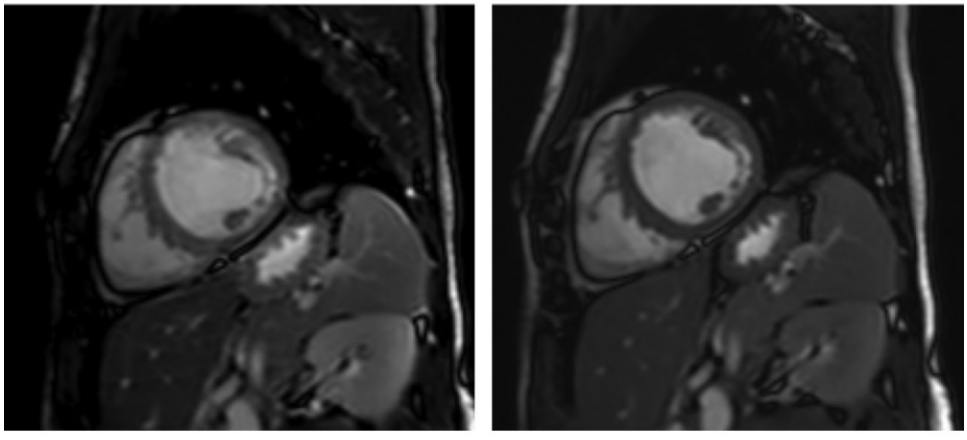

e. f.

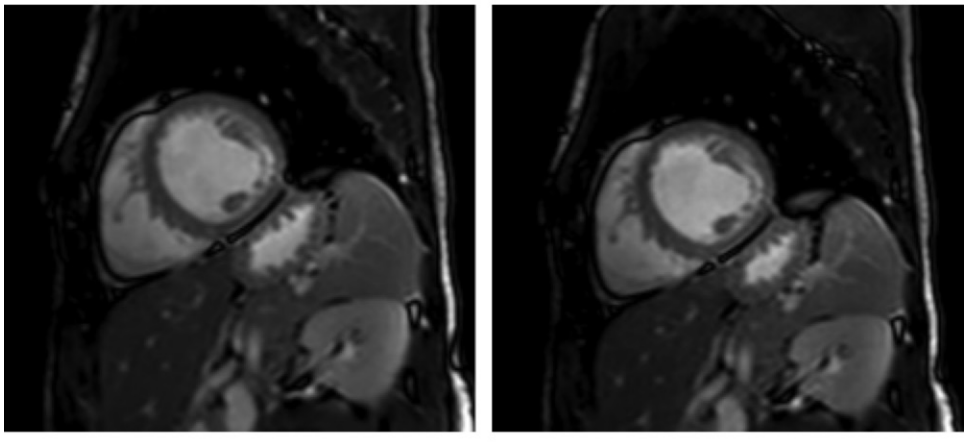

g. h.

flip angle can be decreased, although this comes at the expense of a lower SNR. The TR can be increased; however, this results in higher susceptibility. Using higher degrees of parallel imaging is a possible solution, as this will reduce the number of radiofrequency pulses required because of undersampling, albeit at the cost of lower SNR. Other solutions include the use of refocusing flip-angle modulation techniques such as hyperecho (frequency-selective inversion-recovery), flip-angle sweep (successive reduction of flip angle across echo trains), or variable flip-angle techniques, which can reduce SAR by 2.5–6.0 (1), thus maintaining acceptable SNR or CNR; and using variable-rate selective excitation (VERSE) or tailored radiofrequency pulses, which reduce SAR without decreasing flip angle. In routine practice, use of MR imaging defaults results in automatically slowed acquisition to meet SAR requirements, with adjustments depending on the sequence (eg, increasing echo spacing with FSE-based sequences).

Safety Considerations

The safety profile of devices is different at 3 T than at 1.5 T because of the higher field strength and resonance frequencies. Many devices tested at 1.5 T have not been tested at 3 T. A careful examination of the safety profile should be made before a patient is placed in a 3-T device. Some devices are MR imaging–conditional at 3 T; hence, clinicians must be certain that conditions for safe use of the device are met. The static field poses no higher risk at higher strengths (11); however, increased levels of dizziness and nausea have been reported at 3 T in some studies (12). Higher radiofrequency stimulation such as in nerves or muscles may also be seen at 3 T. In addition, the acoustic noise is higher at 3 T (1).

Magnetohydrodynamic Effect

Magnetohydrodynamic effect refers to the effect of voltage in flowing tissue, such as blood, on the magnetic field. At 3 T, the magnetohydrodynamic effect is amplified. The T waves in the electrocardiographic (ECG) signal appear more prominent than normal and may be mistaken for R waves, which results in erroneous ECG triggering. As a solution, some researchers have suggested the use of a phonoacoustic cardiac-triggering MR imaging stethoscope (13), in which acoustic signals are used instead of the ECG signal. With this technique, an acoustic sensor is placed on the chest to record the heart sounds. The first heart tone of the phonocardiogram indicates the onset of the cardiac cycle, which is then converted by a signal-processing unit into a trigger signal. There is a delay of approximately 30 msec between the R wave of the ECG and the first heart tone. The advantages of using phonocardiography include immunity to magnetohydrodynamic effects, noninterference with electromagnetic fields, and compliance with safety regulations.

Specific Cardiac MR Imaging Sequences at 3 T

The different sequences used at cardiac MR imaging vary in performance. In this section, we review each sequence individually and discuss the advantages and challenges. These are summarized in Table 3.

SSFP Cine Imaging

The SSFP sequence is a workhorse sequence at 1.5-T cardiac MR imaging because of its high SNR and inherent contrast between the myocardial and blood pool signals, which depends on the T2/T1 ratio and rapid image acquisition. The SSFP sequence relies on a steady state of magnetization, in which the longitudinal and transverse magnetizations are at equilibrium; this is achieved with the use of radiofrequency pulses of the same phase and flip angle, at a TR shorter than the T2 of tissue. Unfortunately, use of this critical sequence is often challenging at 3 T. There is an increase in SNR with SSFP sequences at 3 T (approximately 48%), but this increase is limited by a higher T1 and lower T2*. CNR is also increased to a variable amount (14,15). Left ventricle volumetric measurements at 3 T are comparable to those at 1.5 T, but right ventricle measurements are not comparable (16) because of the lower CNR of blood and myocardium at 3 T (17).

Teaching Point

Another major problem of SSFP at 3 T is the higher SAR due to the rapid on-off switching of radiofrequency pulses. This can be limited by decreasing the flip angle and TR; however, these steps further lower the signal intensity and contrast with SSFP sequences. These effects can be mitigated with the use of parallel imaging, which allows higher flip angles at a shorter acquisition time, higher SNR, and higher temporal resolution. Because of increased B_0 inhomogeneities and susceptibility effects at 3 T, there is variability in precession frequencies, which results in phase incoherence and off-resonance banding artifacts, especially at the tissue interface between the myocardium and lung adjacent to the lateral wall of the left ventricle and coronary sinus. When the steady state is disrupted (when the phase angle nears 180°) in a cardiac chamber or blood vessel, flow artifacts are seen (solutions to these problems were discussed earlier). When artifacts are extensive, a GRE cine sequence may instead be used, especially after

Table 3: Important Considerations in the Most Commonly Used Cardiac MR Imaging Sequences

Sequence	Advantages	Disadvantages	Solutions
Cine SSFP	Higher SNR	B_0 inhomogeneity B_1 inhomogeneity Band artifact High SAR	Volume shimming Frequency scout Lower flip angles and TR Parallel imaging
Cine GRE	Less susceptible than SSFP to field inhomogeneities Lower SAR	Blood signal intensity may be lower (high T1 weighting, saturation effects)	Perform after contrast agent administration Long-axis views are better
T1- and T2-weighted images	Higher SNR Higher spatial resolution Improved fat saturation	Longer TR may be needed for T1 weighting	…
First-pass perfusion	Higher SNR Higher CNR High spatial resolution High temporal resolution Lower artifacts	B_1 inhomogeneity Higher T2* effects	GRE readout Saturation-recovery sequences Radiofrequency shimming Adiabatic B_1-insensitive rotation pulses Reduce gadolinium dose Nonenhanced perfusion (BOLD) sequence
MR angiography	Higher SNR Higher CNR Higher spatial resolution Higher temporal resolution Short acquisition time Lower contrast agent dose	Pulmonary perfusion limited because of susceptibility at air-tissue interfaces	…
Delayed enhancement	High SNR High spatial resolution Faster acquisition	Longer inversion times Higher SAR B_1 inhomogeneity	T1 scout Longer recovery available Adiabatic inversion pulses and/or tailored radiofrequency pulses
Coronary artery MR angiography	Higher SNR Higher CNR Higher spatial resolution Improved fat saturation	Low signal with SSFP T2 preparation does not work in reducing myocardial signal B_0 inhomogeneities	Use GRE after intravascular contrast agent administration Use inversion-recovery sequences to suppress myocardial signal Volumetric and/or higher-order shimming
Flow quantification	Higher SNR High spatial resolution High temporal resolution	Overestimation of velocities	…
Myocardial tagging	Higher SNR Higher CNR Tags persist longer because of longer T1	…	…
T2* imaging	Visualization of iron improved	Measurement of iron difficult because of shorter T2* B_0 and B_1 inhomogeneities	T2-based techniques T1 mapping Advanced shimming algorithms
MR spectroscopy	Higher SNR—higher peaks Higher separation of peaks due to higher spectral resolution	…	…

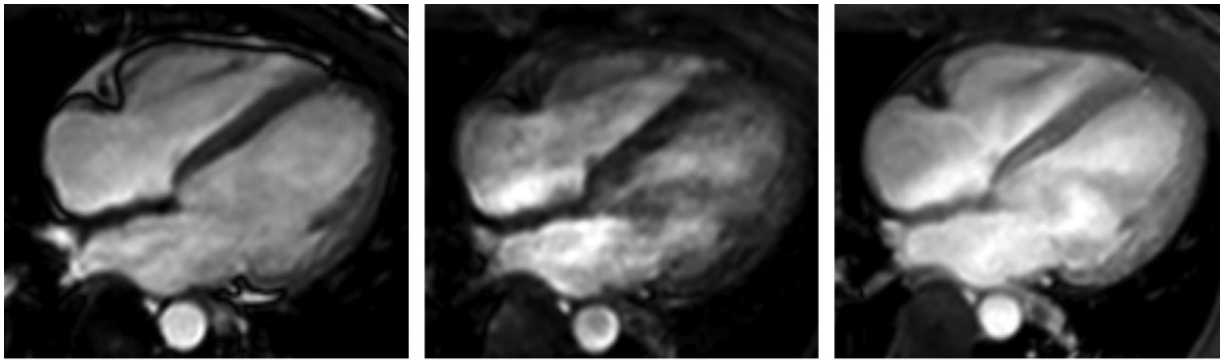

a. b. c.

Figure 11. Comparison of SSFP MR image with GRE images obtained before and after contrast agent administration. **(a)** Four-chamber SSFP MR image shows acceptable SNR and CNR, but artifacts are seen in the left atrial region. **(b)** Nonenhanced GRE MR image obtained at the same level shows lower signal intensity than on the SSFP image (due to inflow effects) but decreased artifacts. **(c)** Contrast-enhanced GRE image obtained at the same level as Movies 1 and 2 shows much higher signal intensity of the blood pool, resulting in higher CNR and SNR than seen on the SSFP image. This technique is an alternative to SSFP when there are extensive band or flow artifacts.

contrast material administration. Overall, SSFP is a sequence where 3 T offers some advantages but also substantial challenges.

GRE Imaging

A spoiled GRE sequence is an alternative option for many clinical scenarios that require SSFP cine images. The signal in this sequence depends on steady-state T1 signal of blood and myocardium. The high signal of blood with GRE sequences is due to T1 shortening of freshly excited spins created by through-plane blood flow. At 1.5 T, the GRE sequence is less preferable than SSFP because of its lower SNR and CNR and dependence on flow. However, with the higher signal available at 3 T, the GRE sequence is in many instances preferred over SSFP (Fig 11a, Movie 1). Although SNR and CNR are higher at 3 T, the blood pool signal at GRE may be lower (Fig 11b, Movie 2) because of the longer T1 of blood at 3 T and saturation effects, especially with short TR or slow flow conditions (ie, lingering blood in the long axis or poor contractility in the long and short axes). Transient signal and flow voids may also be seen with 3-T GRE sequences as a result of inflow phenomenon and unbalanced gradient refocusing; these effects are not seen with SSFP sequences. Contrast with the blood pool can be improved if images are acquired after intravascular contrast material administration (Fig 11c, Movie 3). Long-axis views are improved after contrast material administration because of maintained vascular T1 signal and decreased inflow dephasing artifacts, but no such differences are seen in the short axis (18). Differences in volumes have been shown with precontrast and postcontrast sequences because of improved detection of trabeculations and papillary muscles after contrast agent administration (18). Compared with SSFP sequences, GRE sequences are less sensitive to field inhomogeneities, and SAR is lower as a result of the lower flip angles used.

Black-Blood Imaging

Black-blood images are most commonly used for cardiac and vascular morphologic evaluation, with the nulled blood pool signal allowing for crisp anatomic delineation. Black-blood imaging is also used for tissue characterization in some instances. Black-blood images are improved at 3 T because of higher SNR, which can be traded for higher spatial resolution. Because of the higher T1 at 3 T, the TR for T1-weighted images should be longer, and the TR and TE for T2-weighted images should be shorter compared with at 1.5 T. However, because a longer TR would result in a longer imaging time, TR is typically not changed from that used at 1.5 T. This may result in stronger T1 and T2 weighting at 3 T, which may compensate for the lower dynamic range of T1-weighted images at 3 T (14). Image acquisition times can be decreased by using a lower number of signals, decreasing the number of phase-encoding steps, or using parallel imaging, which may lower SNR (often an acceptable compromise, considering the SNR reserve at 3 T). T2 FSE imaging at 3 T is typically similar to that at 1.5 T. Fat saturation is improved at 3 T because of higher spectral resolution, as discussed earlier.

Dynamic First-Pass Perfusion Imaging

Dynamic first-pass perfusion MR imaging is used to detect myocardial ischemia, which is seen as a perfusion defect on stress images after physiologic or pharmacologic stress. First-pass

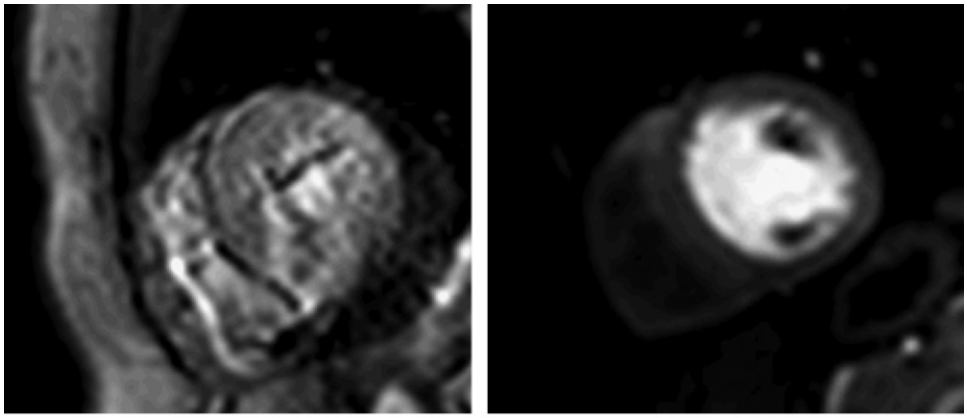

a. b.

Figure 12. Stress perfusion imaging at 1.5 T and 3 T. **(a)** Stress perfusion MR image at 1.5 T shows suboptimal spatial resolution and SNR. **(b)** Stress perfusion MR image at 3 T shows much higher SNR and spatial resolution, with no evidence of any artifact.

perfusion MR imaging has shown high accuracy compared with that of single photon emission computed tomography (SPECT) in several multicenter trials (19). Quantitative methods with this imaging technique are comparable to those with quantitative coronary angiography (20). Perfusion sequences usually include T1-weighted images, SSFP, GRE, or echo-planar imaging incorporating saturation recovery magnetization preparation (21). Perfusion imaging requires high SNR and high spatial and temporal resolutions.

Perfusion sequences are typically more effective at 3 T than at 1.5 T (Fig 12a, Movie 4). The higher SNR at 3 T (up to 109%) (22) can be used to improve spatial or temporal resolution or to increase the use of parallel imaging. The CNR at 3 T is also higher because of the longer T1 of normal myocardium, which improves the contrast between nonperfused and contrast agent–filled myocardium (the T1 of contrast agents does not change). Peak enhancement is also better at 3 T than at 1.5 T (23). The higher spatial resolutions achieved at 3 T may result in decreased size and intensity of the dark rim artifact (Gibbs artifact) at the interface of the myocardial cavity and myocardium (24), a finding that often is confused with pathologic ischemia and is believed to be secondary to low spatial resolution, susceptibility artifact, or motion (Fig 12b, Movie 5). Temporal resolution is also improved at 3 T by using the higher SNR reserve available and by increasing the use of parallel imaging. At 3 T, the diagnostic accuracy of myocardial perfusion imaging of coronary artery stenosis is high (86%), with good correlation with microspheres (25). The GRE readout may be better than with SSFP because of the higher SNR, improved contrast between the blood pool and myocardium, and reduced artifacts. At 3 T, saturation recovery (90° prepulse) is routinely preferred over inversion recovery (180° prepulse) because of consistency and lower rate dependence, insensitivity to arrhythmias, and lower radiofrequency heterogeneity.

The challenges associated with perfusion imaging include increased B_1 inhomogeneities, which result in spatial inhomogeneity and inadequate suppression of background tissue. These factors may be improved by using radiofrequency shimming or adiabatic B_1-insensitive rotation pulses using phase cycling (BIR-04; composite pulse with four segments, with each segment half of the adiabatic inversion pulse; the flip angle is determined by the phase jump between segments two and three and segments one and four) (26), pulse trains, or a 90° adiabatic saturation pulse (27). Higher T2* effects represent another challenge, which can be addressed by reducing the gadolinium chelate dose. Alternatively, nonenhanced perfusion imaging with BOLD sequences is improved at 3 T.

MR Angiography

MR angiography is used to evaluate the vasculature after administration of contrast material. MR angiography is generally improved at 3 T compared with at 1.5 T, as the higher SNR at 3 T can be traded for higher spatial resolution, higher temporal resolution, or shorter acquisition time. The CNR is also higher at 3 T because of the increased difference in T1 between the contrast agent–filled blood vessels and the blood pool before contrast agent administration and the higher contrast between the low T1 of the contrast agent and the high T1 of background tissue at 3 T. Because of the higher SNR, CNR, and spatial resolution at 3 T, a lower dose of contrast agent can be used, which is useful in patients with renal dysfunction (Fig 13a). Further improvements

a. b.

Figure 13. MR angiography at 3 T. **(a)** Coronal maximum intensity projection MR angiogram in a patient with mild renal dysfunction, obtained with a half dose (0.05 mmol/kg) of gadolinium-based contrast agent. Use of 3 T allows acquisition of MR angiograms at lower contrast agent doses because of inherently higher SNR and CNR. **(b)** Sagittal reconstructed MR angiogram obtained in the steady-state phase of intravascular contrast agent administration with a three-dimensional (3D) inversion-recovery navigator-gated sequence shows high SNR and CNR, with suppression of background tissue signal. The use of an intravascular contrast agent allowed ECG gating, which eliminated motion artifacts from the aortic root.

(eg, more rapid image acquisition or improved spatial resolution) can be obtained with parallel imaging. Improved results are also seen with intravascular contrast media with steady-state imaging using inversion-recovery sequences because of the higher SNR, CNR, and T1 of background tissues (Fig 13b). Time-resolved angiographic techniques are also more effective at 3 T because of the higher temporal resolution possible at 3 T (Fig 14, Movie 6). However, at 3 T, pulmonary perfusion may be limited because of higher susceptibility effects at the air-tissue interfaces in the lungs, although the signal in the pulmonary artery is higher (28).

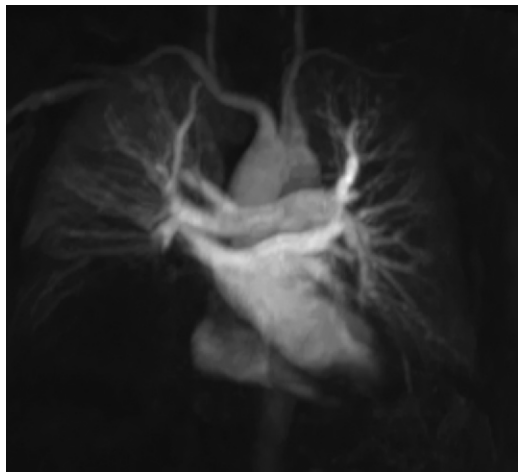

Figure 14. Coronal time-resolved MR angiogram through the thoracic vasculature, obtained at a temporal resolution of 2 seconds, enables visualization of every vascular structure at various time points, with high spatial resolution, SNR, and CNR.

Delayed-Enhancement Imaging

Delayed-enhancement imaging, which is used to evaluate myocardial scar tissue and fibrosis, is performed 10–15 minutes after administration of gadolinium-based contrast agent. Contrast is optimized between normal myocardium and scar tissue through the use of an inversion-recovery pulse, and the image is acquired where the null point is centered on normal myocardium. The higher SNR available at 3 T can be used to generate higher-spatial-resolution images, which allow more precise characterization of scar tissue (Fig 15). At 3 T, improved spatial resolution may be obtained even with single-shot sequences, which typically have limited resolution at 1.5 T (29).

Faster acquisition times are useful in patients who have arrhythmias or who cannot hold their breath. Because of the longer T1 of normal myocardium, the inversion times are different at 3 T than at 1.5 T and can be calculated using a T1 scout (typically 330 msec ± 48 at 3 T and 260 msec ± 30 at 1.5 T [16]) (Fig 16). The contrast between normal and abnormal myocardium is also increased

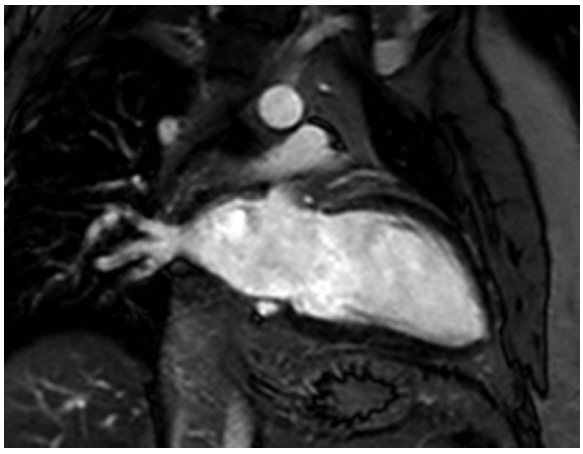

Figure 15. High-quality delayed-enhancement MR image at 3 T shows high SNR and contrast between the nulled myocardium and blood pool.

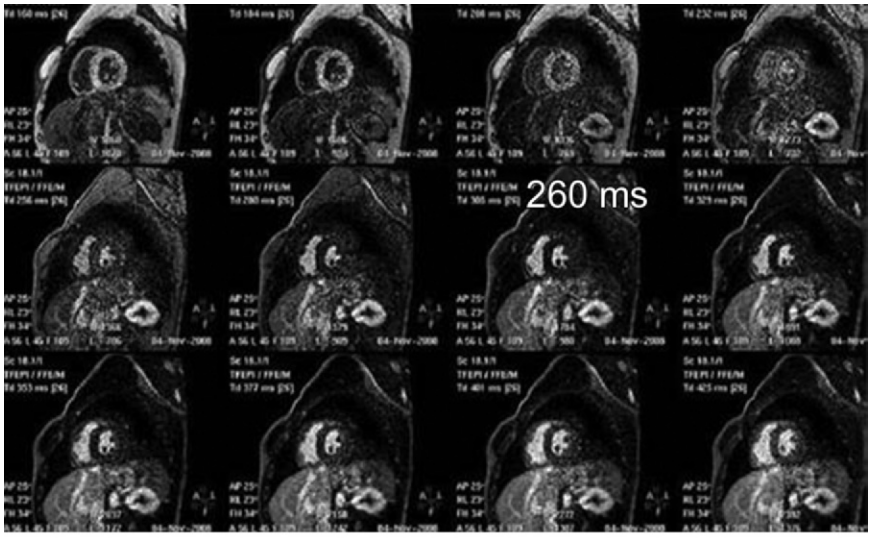

a.

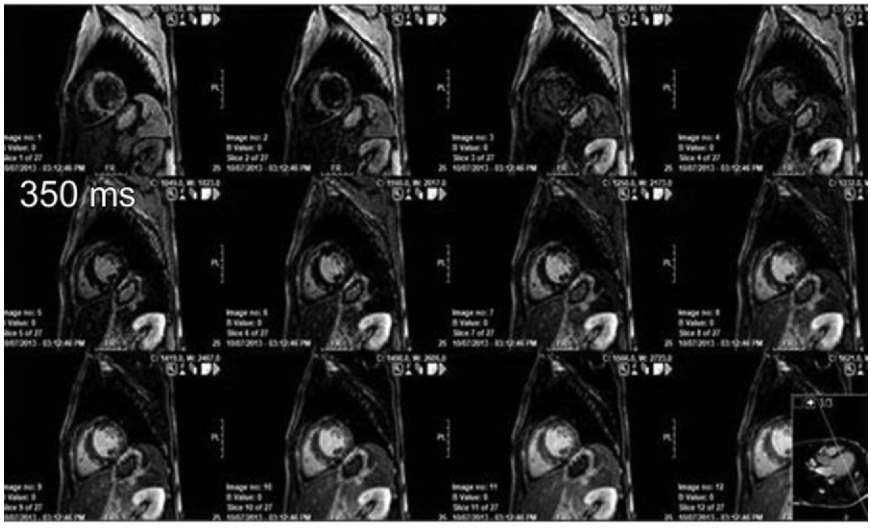

b.

Figure 16. Inversion times at 1.5-T and 3-T MR imaging. **(a)** T1-weighted scout map obtained 10 minutes after contrast agent administration (0.2 mmol/kg) shows myocardial signal intensity at various inversion times at 1.5 T. The optimal myocardial nulling time for this sequence is 260 msec. **(b)** T1-weighted scout map obtained at 3 T demonstrates that the optimal myocardial nulling time is 350 msec. The myocardial nulling time is longer at 3 T because of the longer T1 of myocardium.

at 3-T MR imaging because the T1 of normal myocardium is longer at 3 T and the T1 of contrast agent does not show any substantial difference. At the longer T1 inversion time of myocardium, the scar has much higher signal intensity.

Several studies have demonstrated SNR and CNR up to 3.9 and 3.3 times higher, respectively, at 3 T than at 1.5 T (16,30–32), even with single-shot sequences (29). An important consideration in scar imaging at 3 T is the potential overestimation

Figure 17. Heterogeneous signal suppression. **(a)** Short-axis delayed-enhancement MR images show heterogeneous suppression of the myocardial signal due to B_0 and B_1 field inhomogeneities. **(b)** Short-axis delayed-enhancement MR image obtained in the same patient by using optimal inversion time and an adiabatic inversion pulse shows elimination of the inhomogeneities and homogeneous suppression of the myocardial signal.

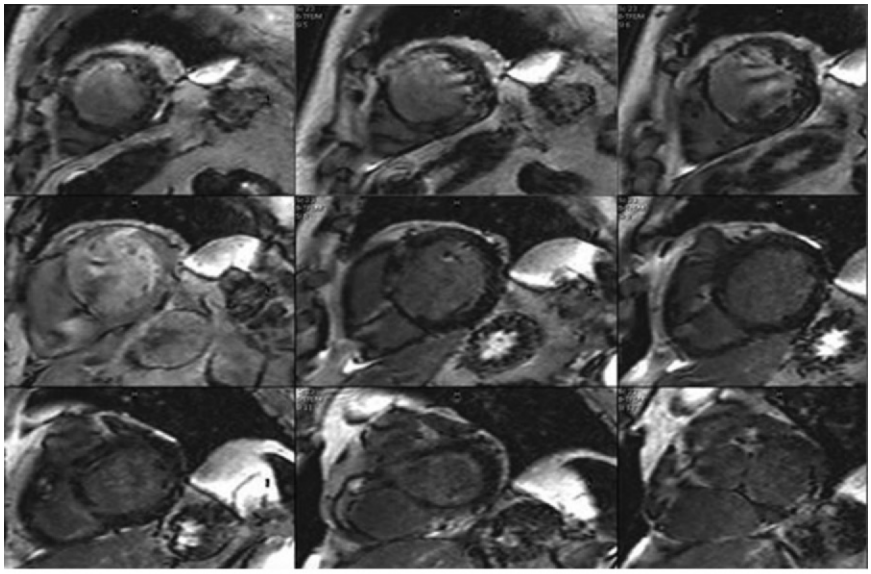

a.

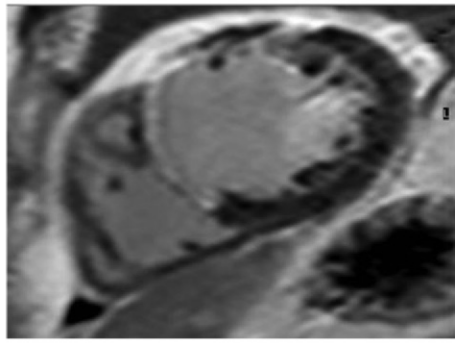

b.

of infarct volume with phase-sensitive inversion-recovery sequences (30). GRE is a preferred readout technique because SSFP is associated with B_0 inhomogeneities and susceptibility artifacts.

The higher radiofrequency power needed for inversion results in a higher SAR, but unlike with other sequences, there is a longer time for recovery between the radiofrequency pulses because they are performed at every other or every third heartbeat. Heterogeneous suppression of myocardial signal can be seen and is due to B_1 inhomogeneities, which result in flip-angle variability (Fig 17a). These inhomogeneities can be overcome with adiabatic inversion pulses (Fig 17b), tailored radiofrequency pulses, or accurate selection of inversion time from a T1 scout.

Coronary MR Angiography

Coronary MR angiography is technically challenging because of the small size of the coronary arteries and the considerable cardiac and respiratory motion that must be accounted for. Coronary MR angiography is now routinely performed using a 3D whole-heart coronary sequence acquired with prospective ECG triggering and respiratory navigation. Fat saturation is used to suppress signal in epicardial fat, and a T2 preparation pulse is used to suppress myocardial signal. At 3 T, 3D whole-heart coronary imaging is potentially better than at 1.5 T because of higher SNR, higher CNR, improved spatial resolution, and improved fat saturation, all of which enable visualization of the distal and side branches, which may be 50% smaller in size (33). SNR and CNR gains of up to 87% and 83%, respectively, have been reported at 3 T (34). At 3 T, 3D whole-heart coronary angiography is more effective when performed with spoiled GRE than with SSFP, particularly after intravascular contrast agent administration and when using centric radial order acquisition (34). At 3 T, SSFP has a lower signal than GRE. T2 preparation (Fig 18a) is not effective in suppressing myocardial signal; hence, an inversion-recovery preparation pulse is used (Fig 18b). As mentioned earlier, the T1 of myocardium is longer at 3 T and can be measured using a T1 scout. With an inversion-recovery sequence and intravascular contrast agent, a 53% higher SNR and a 305% higher CNR have resulted in longer lengths of measurable coronary arteries being reported (34). Improved fat saturation is achieved with spectral frequency sup-

Figure 18. Coronary artery imaging. **(a)** Three-dimensional whole-heart navigator-gated coronary MR angiogram with SSFP at 3 T shows incomplete suppression of the myocardial signal (straight arrow) because of relatively poor performance of a T2-prepared pulse at 3 T. The coronary arteries are visualized (curved arrow). **(b)** Coronary MR angiogram in a different patient after administration of gadolinium contrast agent shows that the signal intensity of the blood pool is higher than it would be without contrast agent administration. There is also improved suppression of the myocardial signal (arrow) with use of an inversion-recovery–prepared pulse. Fat suppression is also improved at 3 T because of higher spectral resolution.

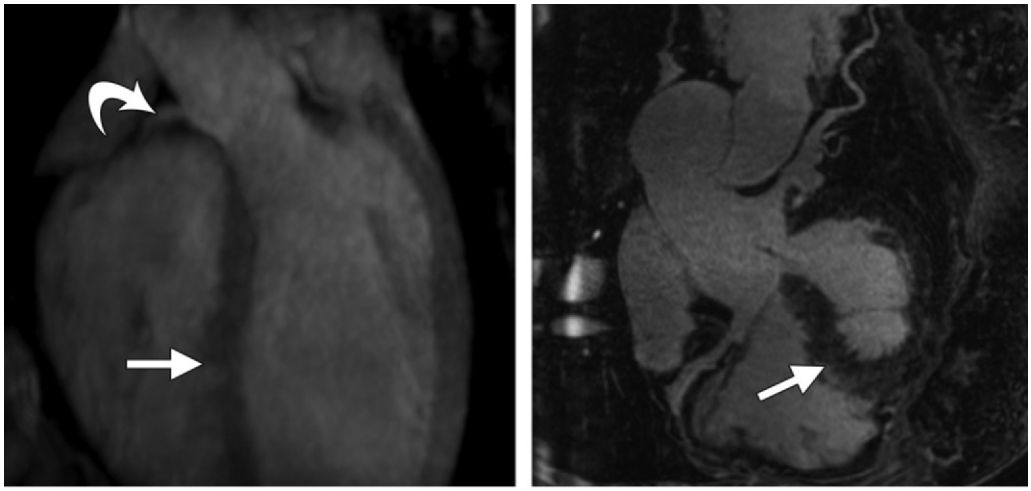

a. b.

pression techniques as a result of higher spectral resolution. Higher spectral resolution can also shorten the fat saturation prepulse, which reduces TE and susceptibility artifacts.

B_0 inhomogeneities are increased because of the higher volume of coverage. These inhomogeneities can be decreased with volumetric shimming, higher-order shim calibration, and a dynamic real-time multisection linear shim. Susceptibility artifacts, which are more prominent along the heart-lung interface and coronary sinus interfaces, can be reduced with proper shimming, lower TE, and shorter readout gradients. Signal variations caused by B_1 inhomogeneities can be addressed with the use of adiabatic radiofrequency pulses (34).

Velocity-encoded Phase-Contrast Flow Quantification

Flow quantification is performed with phase-contrast imaging, in which protons are velocity encoded and the measured phase shift is proportional to the velocity along the direction of a bipolar gradient. Accurate measurement of flow requires high spatial resolution, high temporal resolution, good SNR, measurement orthogonal to the vessel, and appropriate encoded velocity. The use of 3 T can potentially improve the performance of flow quantification in several ways. Increased SNR in the magnitude image corresponds to lower noise in velocity-encoded phase images, which theoretically should result in more accurate measurements. Nonetheless, previous studies of 3 T have shown no effect on measurement of velocity and flow (22,28), and, in fact, some investigators have reported overestimation of velocity compared with phantom models (35). The higher spatial resolution at 3 T enables the evaluation of flow even in small vessels such as coronary arteries. The improved temporal resolution may also allow expanded applications such as evaluation of slow-flow diastolic patterns. A velocity-encoded scout sequence may be performed over a vessel to determine the velocity-encoded value that does not produce aliasing; this value can then be used to obtain the final image.

Myocardial Tagging

Myocardial tagging is useful in the semiautomated evaluation of regional function, using saturation pulses perpendicular to the imaging plane in the form of grids or radial or linear configuration. The saturated magnetization in tag lines depends on T1 relaxation over the cardiac cycle. At 1.5 T, the tag lines fade in diastole because of a shorter T1 (myocardial T1 at 1.5 T, 800–900 msec), and there is incomplete evaluation of diastolic events (Fig 19a, Movie 7). At 3 T, the tag lines persist later into diastole because of a longer T1 (by up to 37%), thereby enabling evaluation of diastolic events (22) (Fig 19b, Movie 8). The higher SNR and CNR of the underlying GRE sequence also allow better tagging at 3 T than at 1.5 T, with improved quantification because of improved border definition (7).

Figure 19. Myocardial tagging. **(a)** Four-chamber 1.5-T MR image in a diastolic phase with myocardial tagging in the form of grids shows that the tag lines have faded, which limits evaluation of diastolic events. **(b)** Four-chamber tagged 3-T MR image shows persistence of the grids throughout the cardiac cycle, which enables more comprehensive evaluation of cardiac events, including diastolic events.

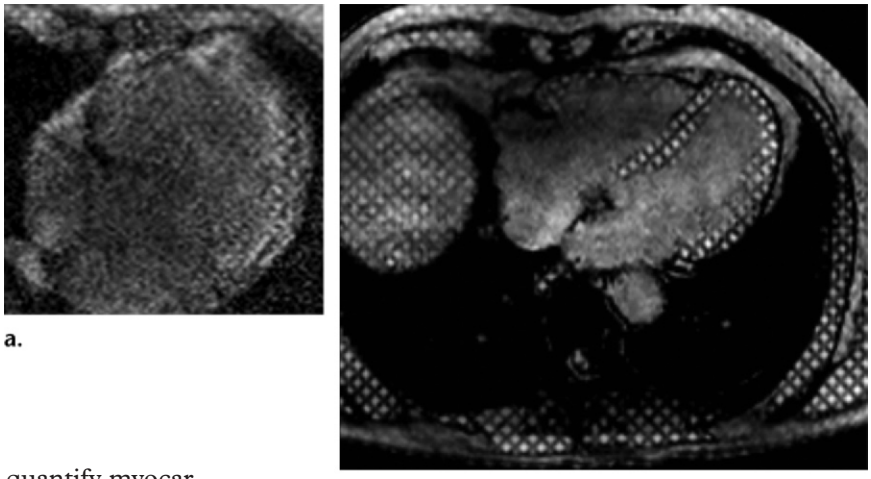

a.

b.

T2* Imaging

T2* imaging, which is used to quantify myocardial iron in patients with thalassemia and other iron-overload conditions, is typically performed with a single breath-hold multiecho GRE sequence. At 1.5 T, a myocardial T2* less than 20 msec correlates with cardiac failure, and a T2* less than 10 msec is associated with severe cardiac dysfunction. At 3 T, because of shorter T2*, qualitative visualization of iron deposition is more obvious as a result of rapid signal decay in iron overload. However, quantification of myocardial iron is challenging because of extensive B_0 and B_1 inhomogeneities and susceptibility effects. In addition, acquisition of the shortest TE and spacing is limited by peak radiofrequency power and gradient strength. Hence, use of 3 T is generally avoided in patients referred for iron quantification. Alternatively, T2 mapping could be used. Although multiecho T2 sequences are generally longer, use of a free-breathing sequence with navigator gating or accelerated techniques may be helpful (36). Other options include T1 mapping and advanced shimming algorithms.

T1 and T2 Mapping

Myocardial T1 and T2 mapping techniques quantify myocardial T1 and T2 relaxation times, are useful in tissue characterization, and are more sensitive for detecting pathologic conditions than are other techniques such as delayed-enhancement and T2-weighted imaging. T1 mapping can be performed with several techniques that produce low-resolution T1-weighted images at different inversion times (eg, modified Look-Locker inversion-recovery [MOLLI] and shortened modified Look-Locker inversion-recovery [ShMOLLI] sequences). Using a nonlinear least-squares curve fitting, T1 values are obtained either before or after contrast agent administration. Extracellular volume can be calculated from postcontrast technique and hematocrit values. With T2 mapping, T2-weighted images are obtained at different TE values, and myocardial T2 is obtained with curve fitting on the basis of a two-parameter equation. Most of these studies have been performed at 1.5 T. The potential advantages of 3 T include high SNR and CNR, which may be used to improve spatial or temporal resolution. The reference values for normal T1 and T2 differ at 3 T, with T1 values longer and T2 values shorter than those at 1.5 T. Higher susceptibility artifacts at 3 T may result in exclusion of some segments and off-resonance or banding artifacts; these artifacts are more commonly seen in the inferolateral left ventricle wall, which unfortunately is a region of interest in conditions such as myocarditis and Fabry disease (37).

MR Spectroscopy

MR spectroscopy is useful in providing metabolic information about myocardial tissues, although this technique remains primarily a research tool. MR spectroscopy is more effective at 3 T than at 1.5 T because of higher SNR, which results in higher peaks and higher spectral resolution, resulting in wider separation between the resonance frequencies of various metabolites.

Vascular Wall Imaging

Imaging of the vascular wall, including the carotid arteries and coronary arteries, has been used for early detection of atherosclerotic plaque and identification of features of plaque vulnerability, such as lipid-rich necrotic core,

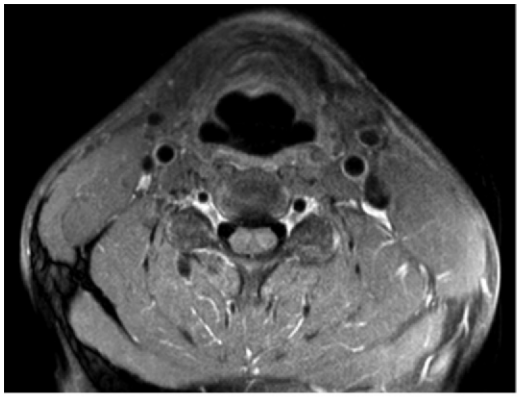

Figure 20. Vessel wall imaging at 3 T. Multicontrast 3-T MR images with different weightings to evaluate vascular plaques include a T1-weighted fat-saturated image **(a)**, a proton-density–weighted image with fat saturation **(b)**, and a T2-weighted image **(c)**. This technique is improved at 3 T because of higher signal.

a.

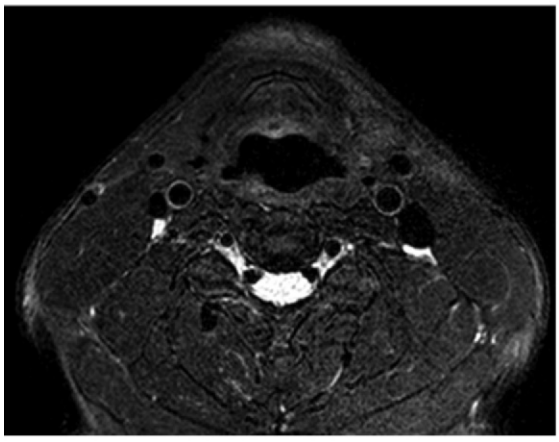

b.

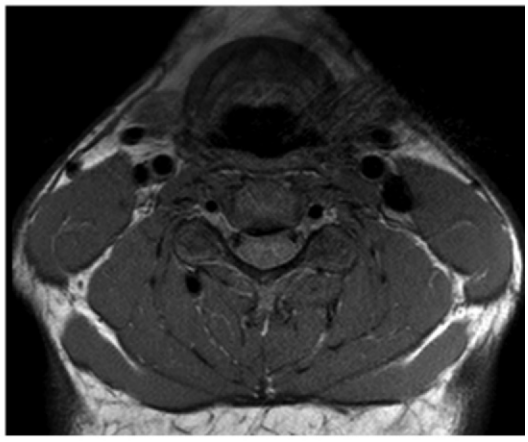

c.

thin fibrous cap, intraplaque hemorrhage, and dynamic contrast agent enhancement. Carotid imaging is performed using multicontrast T1, T2, proton-density–weighted, T1 GRE, or dynamic contrast-enhanced sequences or black-blood MR angiograms, often with specialized coils (Fig 20). Use of 3 T offers the advantages of high SNR and high spatial and temporal resolutions, which make this imaging modality better than 1.5 T for imaging of carotid and coronary arteries. A double inversion-recovery FSE sequence has been associated with an SNR gain of 30% at 3 T (14,38). Other studies have shown SNR increases of up to 223% and CNR increases of up to 225% (39) at 3 T versus 1.5 T, with lower interobserver error at 3 T (40–42). Similar results have also been reported for imaging of the aortic wall (43), especially when a respiratory navigator is used to reduce breathing artifacts. This improved image quality leads to improved plaque-component characterization and reproducibility. The T1 of blood is higher at 3 T; this fact should be used to null the signal from blood in double inversion-recovery sequences, although higher SAR is a consideration. Coronary wall imaging has also been performed using navigator-gated black-blood fast GRE sequences with real-time motion correction or black-blood FSE sequences with breath-hold or free-breathing techniques (44).

Conclusion

Cardiac MR imaging at 3 T improves the performance of several cardiac MR sequences, particularly dynamic first-pass perfusion, MR angiography, myocardial tagging, MR spectroscopy, and fat saturation. Comparable performance to 1.5 T is seen with sequences such as delayed enhancement, flow quantification, and black-blood imaging. SSFP, the workhorse of cardiac MR imaging at 1.5 T, is associated with considerable limitations at 3 T. The main challenges of 3-T cardiac MR imaging include B_0 inhomogeneities, B_1 inhomogeneities, off-resonance band artifacts, susceptibility effects, and chemical shift artifacts. Knowledge of the relevant physics is essential to address these challenging artifacts, optimize cardiac MR imaging sequences, and avoid misdiagnosis.

Acknowledgment.—The authors wish to thank Megan Griffiths, scientific writer at Imaging Institute, Cleveland Clinic, for her editorial input.

References

1. Erturk SM, Alberich-Bayarri A, Herrmann KA, Marti-Bonmati L, Ros PR. Use of 3.0-T MR

imaging for evaluation of the abdomen. RadioGraphics 2009;29(6):1547–1563.
2. Frayne R, Goodyear BG, Dickhoff P, Lauzon ML, Sevick RJ. Magnetic resonance imaging at 3.0 tesla: challenges and advantages in clinical neurological imaging. Invest Radiol 2003;38(7):385–402.
3. Merkle EM, Dale BM. Abdominal MRI at 3.0 T: the basics revisited. AJR Am J Roentgenol 2006;186 (6):1524–1532.
4. Kuhl CK, Träber F, Schild HH. Whole-body high-field-strength (3.0-T) MR imaging in clinical practice. I. Technical considerations and clinical applications. Radiology 2008;246(3):675–696.
5. Sharma P, Socolow J, Patel S, Pettigrew RI, Oshinski JN. Effect of Gd-DTPA-BMA on blood and myocardial T1 at 1.5 T and 3 T in humans. J Magn Reson Imaging 2006;23(3):323–330.
6. Stanisz GJ, Odrobina EE, Pun J, et al. T1, T2 relaxation and magnetization transfer in tissue at 3T. Magn Reson Med 2005;54(3):507–512.
7. Oshinski JN, Delfino JG, Sharma P, Gharib AM, Pettigrew RI. Cardiovascular magnetic resonance at 3.0 T: current state of the art. J Cardiovasc Magn Reson 2010;12:55–67.
8. Deshpande VS, Shea SM, Li D. Artifact reduction in true-FISP imaging of the coronary arteries by adjusting imaging frequency. Magn Reson Med 2003; 49(5):803–809.
9. Sung K, Nayak KS. Measurement and characterization of RF nonuniformity over the heart at 3 T using body coil transmission. J Magn Reson Imaging 2008;27(3):643–648.
10. Bi X, Deshpande V, Simonetti O, Laub G, Li D. Three-dimensional breathhold SSFP coronary MRA: a comparison between 1.5 T and 3.0 T. J Magn Reson Imaging 2005;22(2):206–212.
11. Born M, Tschampa H, Willinek W, Textor H, Kuhl C, Schild H. Prevalence of side effects of MRI at clinical 3 tesla, intraindividual comparison to 1.5 T [abstr]. Radiology 2002;225(P):375.
12. Schenck JF. Safety of strong, static magnetic fields. J Magn Reson Imaging 2000;12(1):2–19.
13. Niendorf T, Sodickson DK, Krombach GA, Schulz-Menger J. Toward cardiovascular MRI at 7 T: clinical needs, technical solutions and research promises. Eur Radiol 2010;20(12):2806–2816.
14. Kuhl CK, Träber F, Gieseke J, et al. Whole-body high-field-strength (3.0-T) MR imaging in clinical practice. II. Technical considerations and clinical applications. Radiology 2008;247(1):16–35.
15. Gutberlet M, Schwinge K, Freyhardt P, et al. Influence of high magnetic field strengths and parallel acquisition strategies on image quality in cardiac 2D CINE magnetic resonance imaging: comparison of 1.5 T vs. 3.0 T. Eur Radiol 2005;15(8): 1586–1597.
16. Klumpp B, Fenchel M, Hoevelborn T, et al. Assessment of myocardial viability using delayed enhancement magnetic resonance imaging at 3.0 tesla. Invest Radiol 2006;41(9):661–667.
17. Hudsmith LE, Cheng AS, Tyler DJ, et al. Assessment of left atrial volumes at 1.5 tesla and 3 tesla using FLASH and SSFP cine imaging. J Cardiovasc Magn Reson 2007;9(4):673–679.
18. Hamdan A, Kelle S, Schnackenburg B, Fleck E, Nagel E. Improved quantitative assessment of left ventricular volumes using TGrE approach after application of extracellular contrast agent at 3 tesla. J Cardiovasc Magn Reson 2007;9(6):845–853.
19. Greenwood JP, Maredia N, Younger JF, et al. Cardiovascular magnetic resonance and single-photon emission computed tomography for diagnosis of coronary heart disease (CE-MARC): a prospective trial. Lancet 2012;379(9814):453–460.
20. Mordini FE, Haddad T, Hsu LY, et al. Diagnostic accuracy of stress perfusion CMR in comparison with quantitative coronary angiography: fully quantitative, semiquantitative, and qualitative assessment. JACC Cardiovasc Imaging 2014;7(1):14–22.
21. Kellman P, Arai AE. Imaging sequences for first pass perfusion: a review. J Cardiovasc Magn Reson 2007;9(3):525–537.
22. Gutberlet M, Noeske R, Schwinge K, Freyhardt P, Felix R, Niendorf T. Comprehensive cardiac magnetic resonance imaging at 3.0 tesla: feasibility and implications for clinical applications. Invest Radiol 2006;41(2):154–167.
23. Araoz PA, Glockner JF, McGee KP, et al. 3 tesla MR imaging provides improved contrast in first-pass myocardial perfusion imaging over a range of gadolinium doses. J Cardiovasc Magn Reson 2005; 7(3):559–564.
24. Di Bella EV, Parker DL, Sinusas AJ. On the dark rim artifact in dynamic contrast-enhanced MRI myocardial perfusion studies. Magn Reson Med 2005;54(5):1295–1299.
25. Christian TF, Bell SP, Whitesell L, Jerosch-Herold M. Accuracy of cardiac magnetic resonance of absolute myocardial blood flow with a high-field system: comparison with conventional field strength. JACC Cardiovasc Imaging 2009;2(9):1103–1110.
26. Kim D, Cernicanu A, Axel L. B_0 and B_1-insensitive uniform T(1)-weighting for quantitative, first-pass myocardial perfusion magnetic resonance imaging. Magn Reson Med 2005;54(6):1423–1429.
27. Shin T, Hu HH, Pohost GM, Nayak KS. Three dimensional first-pass myocardial perfusion imaging at 3 T: feasibility study. J Cardiovasc Magn Reson 2008;10(1):57.
28. Nael K, Saleh R, Nyborg GK, et al. Pulmonary MR perfusion at 3.0 tesla using a blood pool contrast agent: initial results in a swine model. J Magn Reson Imaging 2007;25(1):66–72.
29. Huber A, Bauner K, Wintersperger BJ, et al. Phase-sensitive inversion recovery (PSIR) single-shot True-FISP for assessment of myocardial infarction at 3 tesla. Invest Radiol 2006;41(2):148–153.
30. Bauner KU, Muehling O, Wintersperger BJ, Winnik E, Reiser MF, Huber A. Inversion recovery single-shot TurboFLASH for assessment of myocardial infarction at 3 tesla. Invest Radiol 2007;42 (6):361–371.
31. Ligabue G, Fiocchi F, Ferraresi S, et al. 3-tesla MRI for the evaluation of myocardial viability: a comparative study with 1.5-tesla MRI. Radiol Med (Torino) 2008;113(3):347–362.
32. Stuber M, Botnar RM, Fischer SE, et al. Preliminary report on in vivo coronary MRA at 3 tesla in humans. Magn Reson Med 2002;48(3):425–429.
33. Bi X, Li D. Coronary arteries at 3.0 T: contrast-enhanced magnetization-prepared three-dimensional breathhold MR angiography. J Magn Reson Imaging 2005;21(2):133–139.
34. Kotys MS, Herzka DA, Vonken EJ, et al. Profile order and time-dependent artifacts in contrast-enhanced coronary MR angiography at 3T: origin and prevention. Magn Reson Med 2009;62(2): 292–299.

35. Lotz J, Döker R, Noeske R, et al. In vitro validation of phase-contrast flow measurements at 3 T in comparison to 1.5 T: precision, accuracy, and signal-to-noise ratios. J Magn Reson Imaging 2005;21(5):604–610.
36. Guo H, Au WY, Cheung JS, et al. Myocardial T2 quantitation in patients with iron overload at 3 tesla. J Magn Reson Imaging 2009;30(2):394–400. [Published correction appears in J Magn Reson Imaging 2009;30(5):1230.]
37. von Knobelsdorff-Brenkenhoff F, Prothmann M, Dieringer MA, et al. Myocardial T1 and T2 mapping at 3 T: reference values, influencing factors and implications. J Cardiovasc Magn Reson 2013;15(1):53.
38. Greenman RL, Shirosky JE, Mulkern RV, Rofsky NM. Double inversion black-blood fast spin-echo imaging of the human heart: a comparison between 1.5 T and 3.0 T. J Magn Reson Imaging 2003;17(6):648–655.
39. Koktzoglou I, Chung YC, Mani V, et al. Multislice dark-blood carotid artery wall imaging: a 1.5 T and 3.0 T comparison. J Magn Reson Imaging 2006;23(5):699–705.
40. Alizadeh Dehnavi R, Doornbos J, Tamsma JT, et al. Assessment of the carotid artery by MRI at 3 T: a study on reproducibility. J Magn Reson Imaging 2007;25(5):1035–1043.
41. Syed MA, Oshinski JN, Kitchen C, Ali A, Charnigo RJ, Quyyumi AA. Variability of carotid artery measurements on 3-tesla MRI and its impact on sample size calculation for clinical research. Int J Cardiovasc Imaging 2009;25(6):581–589.
42. Yarnykh VL, Terashima M, Hayes CE, et al. Multicontrast black-blood MRI of carotid arteries: comparison between 1.5 and 3 tesla magnetic field strengths. J Magn Reson Imaging 2006;23(5):691–698.
43. Maroules CD, McColl R, Khera A, Peshock RM. Assessment and reproducibility of aortic atherosclerosis magnetic resonance imaging: impact of 3-tesla field strength and parallel imaging. Invest Radiol 2008;43(9):656–662.
44. Botnar RM, Stuber M, Lamerichs R, et al. Initial experiences with in vivo right coronary artery human MR vessel wall imaging at 3 tesla. J Cardiovasc Magn Reson 2003;5(4):589–594.

Cardiovascular MR Imaging at 3 T: Opportunities, Challenges, and Solutions

Prabhakar Rajiah, MD, FRCR • Michael A. Bolen, MD

RadioGraphics 2014; 34:1612–1635 • **Published online** 10.1148/rg.346140048 • **Content Codes:** CA MR

Page 1613
However, 3-T systems are not without disadvantages, including higher magnetic field and radiofrequency inhomogeneities; higher incidence of susceptibility, off-resonance, and chemical shift artifacts; and higher radiofrequency deposition resulting in a higher specific absorption rate (SAR).

Page 1613
Cardiac MR imaging at 3 T results in higher SNR, higher resonance frequency, increased in-phase periodicity, and altered relaxation times, all of which have a substantial effect on the performance and quality of cardiac MR imaging.

Page 1615
The challenges of 3-T cardiac MR imaging include B_0 inhomogeneities and consequent band, flow, and susceptibility artifacts; B_1 inhomogeneities and consequent field-focusing and dielectric resonance effects; and chemical shift artifacts.

Page 1622
Conveniently, 3 T improves the use of parallel imaging, and parallel imaging improves the use of 3 T.

Page 1624
The SSFP sequence relies on a steady state of magnetization, in which the longitudinal and transverse magnetizations are at equilibrium; this is achieved with the use of radiofrequency pulses of the same phase and flip angle, at a TR shorter than the T2 of tissue. Unfortunately, use of this critical sequence is often challenging at 3 T.